Deletion of FNDC5/Irisin modifies murine osteocyte function in a sex-specific manner

Anika Shimonty[1], Fabrizio Pin[2], Matt Prideaux[2], Gang Peng[3], Joshua R Huot[2], Hyeonwoo Kim[4], Clifford J Rosen[5], Bruce M Spiegelman[6], Lynda F Bonewald[7*]

[1]Indiana Center for Musculoskeletal Health, School of Medicine, Indiana University, IN, 46202, Indianapolis.

[2]Indiana Center for Musculoskeletal Health, Department of Anatomy, School of Medicine, Indiana University, IN, 46202, Indianapolis.

[3]Indiana Center for Musculoskeletal Health, Department of Medicine and Molecular Genetics, School of Medicine, Indiana University, IN, 46202, Indianapolis.

[4]Department of Biological Sciences, Korea Advanced Institute of Science and Technology, Daejeon, South Korea.

[5]Maine Medical Center Research Institute, ME, 04074, Scarborough, USA.

[6]Department of Cancer Biology, Dana Farber Cancer Institute and Department of Cell Biology, Harvard University Medical School, MA, 02115, Boston, USA.

[7]Department of Anatomy, Cell Biology and Physiology, Orthopaedic Surgery, School of Medicine, Indiana Center for Musculoskeletal Health, Indiana Center for Musculoskeletal Health, Indiana University, IN, 46202, Indianapolis.

***For correspondence:**

lbonewal@iu.edu (LB)

Abstract

Irisin, released from exercised muscle, has been shown to have beneficial effects on numerous tissues but its effects on bone are unclear. We found significant sex and genotype differences in bone from wildtype (WT) mice

compared to mice lacking *Fndc5* (KO), with and without calcium deficiency. Despite their bone being indistinguishable from WT females, KO female mice were partially protected from osteocytic osteolysis and osteoclastic bone resorption when allowed to lactate or when placed on a low-calcium diet. Male KO mice have more but weaker bone compared to WT males, and when challenged with a low-calcium diet lost more bone than WT males. To begin to understand responsible molecular mechanisms, osteocyte transcriptomics was performed. Osteocytes from WT females had greater expression of genes associated with osteocytic osteolysis and osteoclastic bone resorption compared to WT males which had greater expression of genes associated with steroid and fatty acid metabolism. Few differences were observed between female KO and WT osteocytes, but with a low calcium diet, the KO females had lower expression of genes responsible for osteocytic osteolysis and osteoclastic resorption than the WT females. Male KO osteocytes had lower expression of genes associated with steroid and fatty acid metabolism, but higher expression of genes associated with bone resorption compared to male WT. In conclusion, irisin plays a critical role in the development of the male but not the female skeleton and protects male but not female bone from calcium deficiency. We propose irisin ensures the survival of offspring by targeting the osteocyte to provide calcium in lactating females, a novel function for this myokine.

In-text word count (Introduction, Results, and Discussion): 6950

Number of data elements: 1 table, 6 figures.

Introduction

It is widely accepted that bone and muscle interact mechanically as movement of the skeleton by muscle is essential for life. Less well-known but becoming more generally accepted is that muscle and bone can communicate through secreted factors ***Brotto and Bonewald*** (***2015***); ***Bonewald*** (***2019***). Muscle produces factors such as *β*-aminoisobutyric Acid (BAIBA) and irisin with exercise, that have positive effects on bone, adipose tissue, brain, and other organs, whereas sedentary muscle produces factors such as myostatin that has negative effects on

both bone and muscle ***Brotto and Bonewald*** (***2015***); ***Karsenty and Mera*** (***2018***); ***Kitase et al.*** (***2018***); ***Bostrom et al.*** (***2012***); ***Hamrick et al.*** (***2006***).

Many of the factors secreted by bone are produced by osteocytes, the most abundant and the longest-living bone cell ***Bonewald*** (***2011***); ***Dallas et al.*** (***2013***). These cells are derived from terminally differentiated osteoblasts that become surrounded by the newly mineralizing bone matrix ***Dallas et al.*** (***2013***). Osteocytes are multifunctional and appear to be the major mechanosensory cell in bone ***Bonewald*** (***2011***); ***Temiyasathit and Jacobs*** (***2010***); ***Uda et al.*** (***2017***). Under unloaded conditions, these cells produce sclerostin, a negative regulator of bone formation and Receptor Activator of Nuclear factor Kappa β ligand (RANKL), the major factor that recruits and activates osteoclasts to resorb bone ***Nakashima et al.*** (***2011***); ***Xiong and O'Brien*** (***2012***); ***Xiong et al.*** (***2015***); ***Ono et al.*** (***2020***). In contrast, with anabolic mechanical loading, these cells produce factors such as prostaglandin E2 (PGE_2) that have positive effects on myogenesis and muscle function ***Mo et al.*** (***2015***). Osteocytes play a major role in mineral metabolism, through regulation of both calcium and phosphate homeostasis. Osteocytes secrete Fibroblast Growth Factor 23 to target the kidney to regulate phosphate excretion. Both Parathyroid Hormone (PTH) and Parathyroid related peptide (PTHrP) regulate calcium homeostasis via the PTH type 1 receptor on osteocytes ***Feng et al.*** (***2009***); ***Teti and Zallone*** (***2009***). Under the physiological calcium-demanding condition of lactation, osteocytes respond to PTHrP by removing their surrounding perilacunar matrix to provide calcium for offspring, and upon weaning this perilacunar matrix is rapidly replaced, a process referred to as perilacunar remodeling ***Qing and Bonewald*** (***2009***); ***Qing et al.*** (***2012***); ***Wysolmerski*** (***2013***). However, under pathological conditions such as ovariectomy, hyperparathyroidism, hypophosphatemic rickets, and cancer, excessive removal of their perilacunar matrix occurs through osteocytic osteolysis ***Tsourdi et al.*** (***2018***); ***Jähn-Rickert and Zimmermann*** (***2021***); ***Pin et al.*** (***2021***); ***Shimonty et al.*** (***2023***).

Bone is the largest calcium reservoir in the body and human mothers can lose an average of 250 mg/day of calcium in milk, emphasizing the need for a calcium-replete diet to prevent bone loss ***Qing et al.*** (***2012***); ***Wysolmerski*** (***2002***); ***Kalkwarf*** (***2004***). During lactation, PTHrP targets the osteocyte to elevate genes coding for factors necessary for the removal of their calcium-ladened perilacunar matrix and to increase RANKL as an activator of osteoclasts ***Kovacs***

(***2001***). During lactation, RANKL targets osteoclasts, thereby driving osteoclastic bone resorption. Osteocytic osteolysis is accomplished through the expression of 'osteoclast-specific' genes such as cathepsin K (*Ctsk*), tartrate-resistant acid phosphatase (TRAP, gene *Acp5*), and carbonic anhydrase 1 (*Car 1*) ***Qing and Bonewald*** (***2009***); ***Qing et al.*** (***2012***). In addition, there is an increase in genes coding for the proton pumps, ATPase H^+ Transporting V1 Subunit G1 (*Atp6v1g1*) and ATPase H^+ Trans- porting V0 Subunit D2 (*Atp6v0d2*) necessary to dissolve and remove calcium from bone collagen ***Jahn*** (***2017***).

Systemic calcium deficiency such as a decrease in dietary calcium triggers an increase in PTH, acting to mobilize calcium from bones to maintain normal homeostatic circulating calcium levels ***Goltzman*** (***2008***). Worldwide, over 3.5 billion people suffer from dietary calcium deficiency, and women are at a higher risk of this condition ***Kumssa et al.*** (***2015***); ***Body et al.*** (***2016***). Aging often results in hypocalcemia and bone loss due to low vitamin D, hypoparathyroidism, genetic abnormalities, medications decreasing dietary calcium absorption, and menopause in women. Calcium deficiency can lead to osteopenia, osteoporosis, and increased fracture risk, primarily due to secondary hyperparathyroidism ***Kumssa et al.*** (***2015***); ***Body et al.*** (***2016***).

Irisin is a recently discovered myokine generated in response to exercise when Fibronectin type III Domain Containing protein 5 (FNDC5) is proteolytically cleaved by a yet undetermined protease ***Bostrom et al.*** (***2012***). FNDC5 is expressed in the heart, kidney, testes, brain, and other tissues; however, skeletal muscle appears to be the primary producer ***Erickson*** (***2013***); ***Maak et al.*** (***2021***); ***Tsourdi et al.*** (***2022***). Cleaved irisin circulates to distant organs, such as adipose tissue where irisin increases a thermogenic gene program, including the expression of uncoupling protein 1 (UCP1) in a process referred to as browning. This is associated with increased energy expenditure and improvement in glucose tolerance, both of which are important for the prevention of Type 2 diabetes and the reduction of complications from obesity ***Perakakis et al.*** (***2017***); ***Korta et al.*** (***2019***). Irisin can also regulate glucose uptake in skeletal muscle ***Lee et al.*** (***2015***), and increases myogenesis and oxidative metabolism, responsible for increasing skeletal muscle mass ***Colaianni and Grano*** (***2015***). Irisin also plays an important positive role in cognitive functions with exercise, aging, and degenerative diseases such as Alzheimer's disease (AD) and Parkinson's disease

131 (PD) ***Islam et al.*** (***2021***). Using the tail-vein injection method to deliver
132 exogenous irisin, it was shown that irisin can cross the blood-brain barrier
133 ***Islam et al.*** (***2021***).

134 Results from studies regarding the effects of irisin on bones are complex and
135 somewhat contradictory. Colaianni et al have shown that recombinant irisin exerts
136 a beneficial effect on cortical bones in young male mice by reducing the secretion
137 of osteoblast inhibitors and increasing the activity of osteogenic cells ***Colaianni et***
138 ***al.*** (***2015***). However, another study has shown that recombinant irisin treatment
139 of MLO-Y4 osteocyte-like cells induces gene and protein level expression of
140 *Sost*/sclerostin, a negative regulator of bone formation while maintaining cell
141 viability under oxidative stress ***Kim et al.*** (***2018***). Rosen et al. have shown using
142 female FNDC5 overexpressing female mice that irisin acts directly acts on
143 osteoclast progenitors to increase differentiation and promote bone resorption
144 ***Estell et al.*** (***2020***). Kim et al. have shown that 9-month-old ovariectomized
145 FNDC5 global KO mice are protected against ovariectomy-induced trabecular
146 bone loss through the inactivation of osteocytic osteolysis and osteoclastic
147 bone resorption ***Kim et al.*** (***2018***). The majority of these studies used only male
148 or female mice, suggesting a sex-dependent response may be responsible for
149 these seemingly opposing findings ***Estell et al.*** (***2020***); ***Colaianni et al.*** (***2017***);
150 ***Kawao et al.*** (***2018***); ***Ma et al.*** (***2018***); ***Colucci et al.*** (***2019***); ***Posa et al.*** (***2021***).

151 As shown previously, FNDC5 deletion has a protective effect against ovariectomy-
152 induced bone loss via a reduction of osteocytic osteolysis and osteoclastic
153 resorption ***Kim et al.*** (***2018***). We, therefore, hypothesized that FNDC5 deletion
154 would also be protective against bone loss due to calcium deficiency that occurs
155 with lactation and a calcium-deficient diet. Our data show that the female
156 skeleton in FNDC5 null female mice was resistant to bone loss due to both
157 lactation and low calcium. However, for FNDC5 null males, deletion not only
158 failed to protect but exacerbated bone loss in response to low calcium. We
159 propose that male and female osteocytes respond to irisin differently under
160 calcium-demanding conditions based on the divergence of the male and female
161 osteocyte transcriptome with sexual maturity when the female osteocyte must
162 serve a critical role in reproduction.

Results

With lactation, FNDC5 global KO mice lose less bone and are mechanically stronger compared to WT

No significant differences were observed in either bone composition or morphometry between 4-5-month-old virgin WT and FNDC5 global KO female mice (Fig 1A, 1B, 1C, sup table 1), showing that the absence of FNDC5/irisin does not affect female bone development. It has been previously shown that during lactation, maternal bones release calcium to supplement milk, especially in response to the large calcium demand induced by large litter size or a calcium- deficient diet ***Wysolmerski*** (***2002***); ***Ardeshirpour et al.*** (***2015***). Similar to previous studies, 2 weeks of lactation resulted in bone loss in both WT and KO mice, with a significant reduction in cortical bone area (Ct. B.Ar), cortical bone area fraction percentage (Ct.B.Ar/T.Ar%), and cortical thickness (Ct. Th) (Fig 1A, 1B) as well as bone mineral density, BMD (Fig 1C). However, the KO mice lost less bone com- pared to the WT mice, as evidenced by the significantly higher bone area fraction percent, cortical thickness, and BMD (Fig. 1A, 1B, 1C) as well as the lower percentage of bone loss (Sup Table 1). These data suggest that the FNDC5 KO mice are more resistant to the effects of calcium demand. Analysis of trabecular bone parameters including trabecular bone volume fraction (BV/TV), trabecular thickness (Tb. Th), trabecular spacing (Tb. Sp), and trabecular number (Tb. N) showed no significant difference in bone loss between lactating WT and lactating KO mice (Sup table 1).

Bone loss can have significant effects on bone mechanical properties including bone strength, stiffness, and fragility. To determine mechanical properties, 3-point bending tests were performed on mice femurs. There was no significant difference between virgin WT and KO mice in terms of ultimate force and stiffness (Fig. 1D). However, femurs from the lactating KO mice were stronger than lactating WT, as evidenced by the higher stiffness and significantly higher ultimate force needed to break the bone (Fig 1D, Sup Table 1, Table 2). This data indicates that lactating KO female bone retains greater resistance to fracture than lactating WT mice by less lactation-induced bone loss.

198

199 **With lactation, FNDC5 global KO mice have fewer TRAP-positive osteo-**
200 **clasts and osteocytes as well as smaller osteocyte lacunar area compared**
201 **to WT mice**

202 Previously it was shown that lactation-induced bone loss occurs via not only
203 osteoclastic bone resorption but also osteocytic osteolysis *Qing et al* (*2012*). To
204 determine the relative contribution of each means of resorption, tibial
205 longitudinal sections were stained for tartrate-resistant acid phosphatase TRAP-
206 positive multinucleated osteoclasts as well as TRAP-positive osteocytes.

207 Virgin FNDC5 KO female mice had fewer TRAP-positive osteocytes compared
208 to virgin WT mice (Fig. 1E, 1G). This is the first and only difference we have
209 observed between WT and KO female mice and suggests that the osteocytes in
210 the female KO mice are less 'primed' to initiate osteocytic osteolysis. With
211 lactation, TRAP-positive osteocytes significantly increased in both WT and KO
212 mice (Fig 1G, Supplementary Table 2). Virgin KO mice started with a lower number
213 of TRAP- positive osteocytes compared to virgin WT, and with lactation, their
214 number of TRAP-positive osteocytes was still significantly lower compared to
215 lactating WT (Fig. 1G).

216 During lactation, in response to calcium demand, osteocytes can remove their
217 perilacunar matrix. This process is similar but not identical to osteoclastic bone
218 resorption *Tsourdi et al.* (*2018*); *Bélanger* (*1969*); *Wysolmerski* (*2012*) as
219 osteoclasts generate resorption pits, whereas osteocytes increase their lacunar
220 size *Qing et al.* (*2012*); *Wysolmerski* (*2013*). We measured the osteocyte lacunar
221 area and found no significant difference between virgin WT and KO female
222 mice (Fig. 1F, 1H) even though the KO females have fewer TRAP-positive
223 osteocytes (Fig. 1G). With lactation, the lacunar area increased in both groups;
224 however, KO mice had significantly smaller average lacunar area compared to
225 WT (Fig. 1H). These data show that female lactating FNDC5 KO mice undergo
226 less osteocytic osteolysis compared to WT females under the calcium-
227 demanding condition of lactation.

228 In virgin mice, there were no significant differences in osteoclast number per
229 bone perimeter (Oc/B.Pm) between WT and KO female mice (Fig 1I). With
230 lactation, osteoclast number increased in both groups, however, KO mice had
231 significantly fewer osteoclasts (Fig 1I) and a significantly lower percentage
232 increase in the number of osteoclasts compared to WT (Supplementary Table

1). This suggests that with lactation, fewer osteoclasts are activated in the KO as compared to the WT mice.

RANKL, another major player in bone resorption ***Xiong and O'Brien*** (***2012***), is also increased during lactation to induce osteoclastic bone resorption ***Ardeshirpour et al.*** (***2015***) by osteocytes, the major source of RANKL ***Nakashima et al.*** (***2011***); ***Xiong and O'Brien*** (***2012***); ***Ono et al.*** (***2020***). Virgin WT and KO mice had comparable serum RANKL levels (Fig. 1J). With lactation, the increase in serum RANKL was significant in the WT mice, but not in the KO mice (Fig. 1I, Sup Table 1).

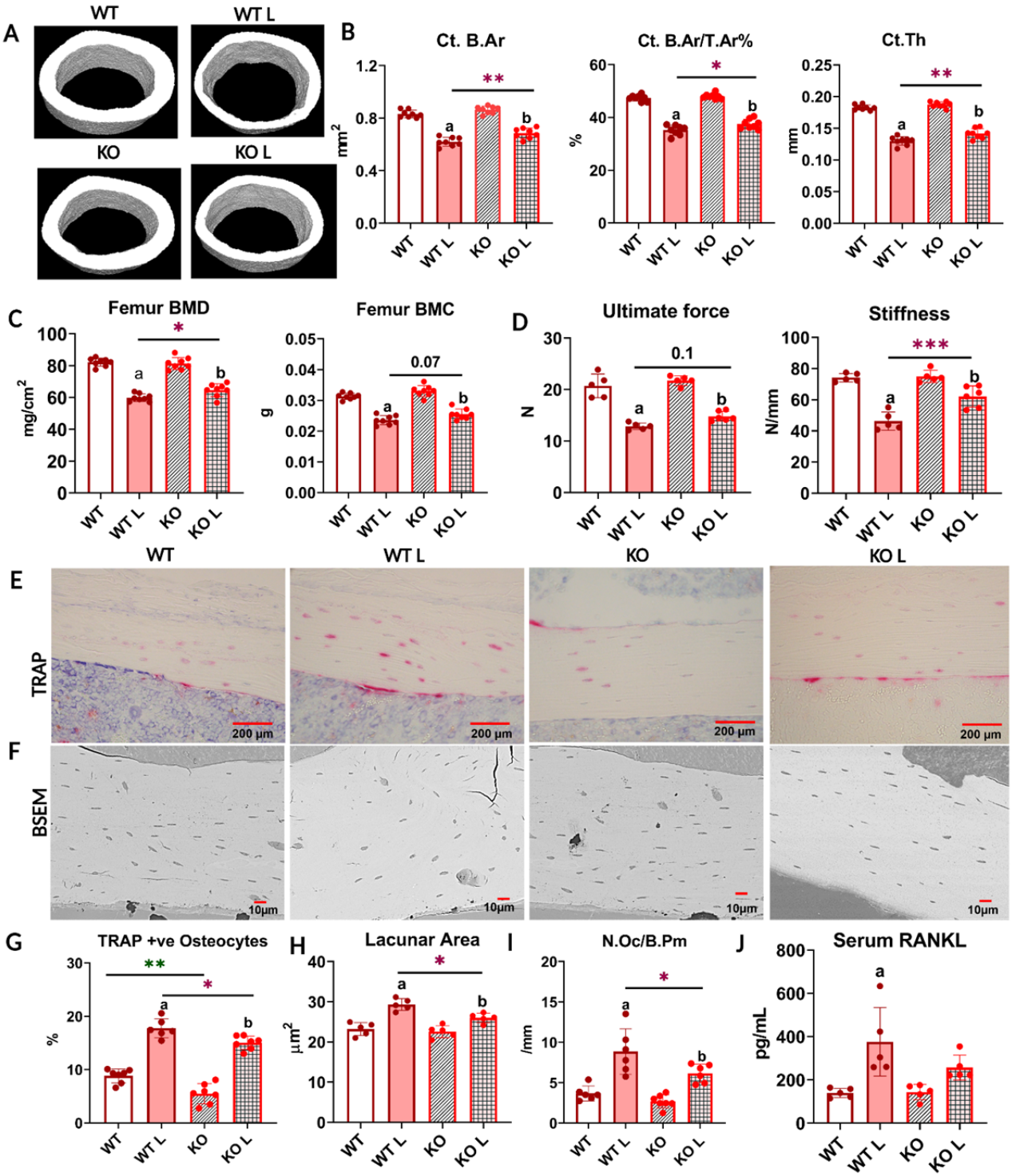

Fig 1: With lactation, FNDC5 global KO mice lose less bone and are mechanically stronger compared to WT

A: Respective μCT images of femoral midshafts from WT virgin (WT), KO virgin (KO), WT lactation (WT L), and KO lactation (KO L) mice.

B: μCT analysis of femoral cortical bone parameters of virgin and lactating WT and KO female mice reported as cortical bone area (Ct. B.Ar), cortical bone area fraction (Ct. B.Ar/ T.Ar %), and cortical thickness (Ct. Th).

266 **C:** Ex vivo DXA analysis for BMD and BMC of femurs from virgin and lactating WT and KO
267 female mice.
268 **D:** 3-point bending analysis of WT and KO virgin and lactating mice reported as
269 ultimate force and stiffness.
270 **E:** Representative TRAP-stained images of cortical bone from WT virgin (WT), WT lactation
271 (WT L), KO virgin (KO), and KO lactation (KO L) mice.
272 **F:** Representative backscatter scanning electron microscope (BSEM) images of WT virgin
273 (WT), KO virgin (KO), WT lactation (WT L), and KO lactation (KO L) mice femur at 400X
274 magnification.
275 **G:** Percent TRAP-positive osteocytes (TRAP +ve) in tibia from virgin and lactating WT and
276 KO mice.
277 **H:** Average osteocyte lacunar area in femurs from virgin and lactating WT and mice.
278 **I:** Osteoclast number per bone perimeter in tibia from virgin and lactating WT and KO
279 mice.
280 **J:** Serum RANKL levels in virgin and lactating WT and KO mice.
281 4-5-month-old WT and KO virgin and lactating mice, n= 5-8/group. a= Significantly different
282 from WT, b= Significantly different from KO, *= $p< 0.05$, **= $p< 0.01$, ***= $p< 0.001$. 2-way
283 ANOVA with Tukey's post hoc test was performed for statistical analysis.
284
285 **FNDC5 KO female and male bone have opposite responses to a low-**
286 **calcium diet**
287 After observing that bones are protected against lactation-induced bone loss
288 in FNDC5/irisin KO female mice, we sought to determine if FNDC5/irisin null (KO)
289 male bone is protected from calcium deficiency. Therefore, both female and
290 male mice were placed on a calcium-deficient diet for 2 weeks to induce bone
291 loss.
292 With regards to the female mice, similar results were observed with the low
293 calcium diet as was observed with lactation. WT and KO female mice showed no
294 significant differences in their BMD and BMC (Supplementary Table 2), as well as
295 no differences in either cortical (Fig 2B) or trabecular bone parameters
296 (Supplementary Table 3). After 2 weeks of a low calcium diet, both WT and KO
297 female mice lost bone as can be evidenced by decreased BMD
298 (Supplementary Table 2) and bone area fraction (Fig 2B), however similar to
299 the lactation experiment, the KO female mice were partially resistant to bone
300 loss compared to the female WT mice given a low calcium diet (Fig 2A, B).

301 Interestingly a higher marrow cavity area was observed in the WT compared to
302 the KO, unlike the lactation experiment (Supplementary Table 2). Mechanical
303 testing showed that bone from female KO mice required a significantly higher
304 force to break, and thus were stronger com- pared to WT females given a low
305 calcium diet (Fig 2C). Therefore, similar to the calcium-demanding conditions
306 of lactation, on a low calcium diet, the female KO bone is more resistant to bone
307 loss than WT.

308 Unlike female bone, significant differences were observed between WT and
309 KO male bone. KO male mice on a normal diet had a significantly higher BMD,
310 BMC (Supplementary Table 2), and bone area fraction compared to WT males
311 of the same age (Fig 2E). However, femurs from KO mice had significantly lower
312 stiffness than WT (Fig 2F), indicating a difference in the material properties of the
313 bone. Therefore, the KO males have larger, denser, but weaker bones compared
314 to WT males. To determine the effect of calcium deficiency on male mice, KO
315 and WT mice were subjected to a low-calcium diet for 2 weeks. Unlike the
316 female KO mice which were protected from the effects of a low calcium diet,
317 the KO male mice had an opposite response. The male KO mice had greater
318 bone loss compared to the WT male mice (Fig 2D, E, Table 2), the trabecular
319 bone loss followed the same trends but was not statistically significant
320 (Supplementary Table 2), and the femurs from the KO male mice were
321 significantly less stiff and therefore weaker compared to the WT males on a low
322 calcium diet (Fig 2F). This data shows a sex-specific response to low calcium.

323 To ensure that the effects observed in the KO mice were due to circulating
324 irisin, and not FNDC5 deletion, we injected AAV8- irisin in KO male mice, with
325 AAV8-GFP as the control, and placed them on the same low Ca diet. We chose
326 male mice due to the highly significant effect we saw in the KO males compared
327 to WT males on a low-calcium diet. The irisin injection rescued the phenotype
328 in KO male mice, shown by the higher cortical bone area fraction and the lower
329 endosteal perimeter (Fig 2G). There was a tendency for higher ultimate force and
330 stiffness in the KO males that received the AAV8-irisin injection, however, this
331 did not reach statistical significance (Fig 2H). These data show that the observed
332 effects in the FNDC5 null animals are due to an absence of irisin.

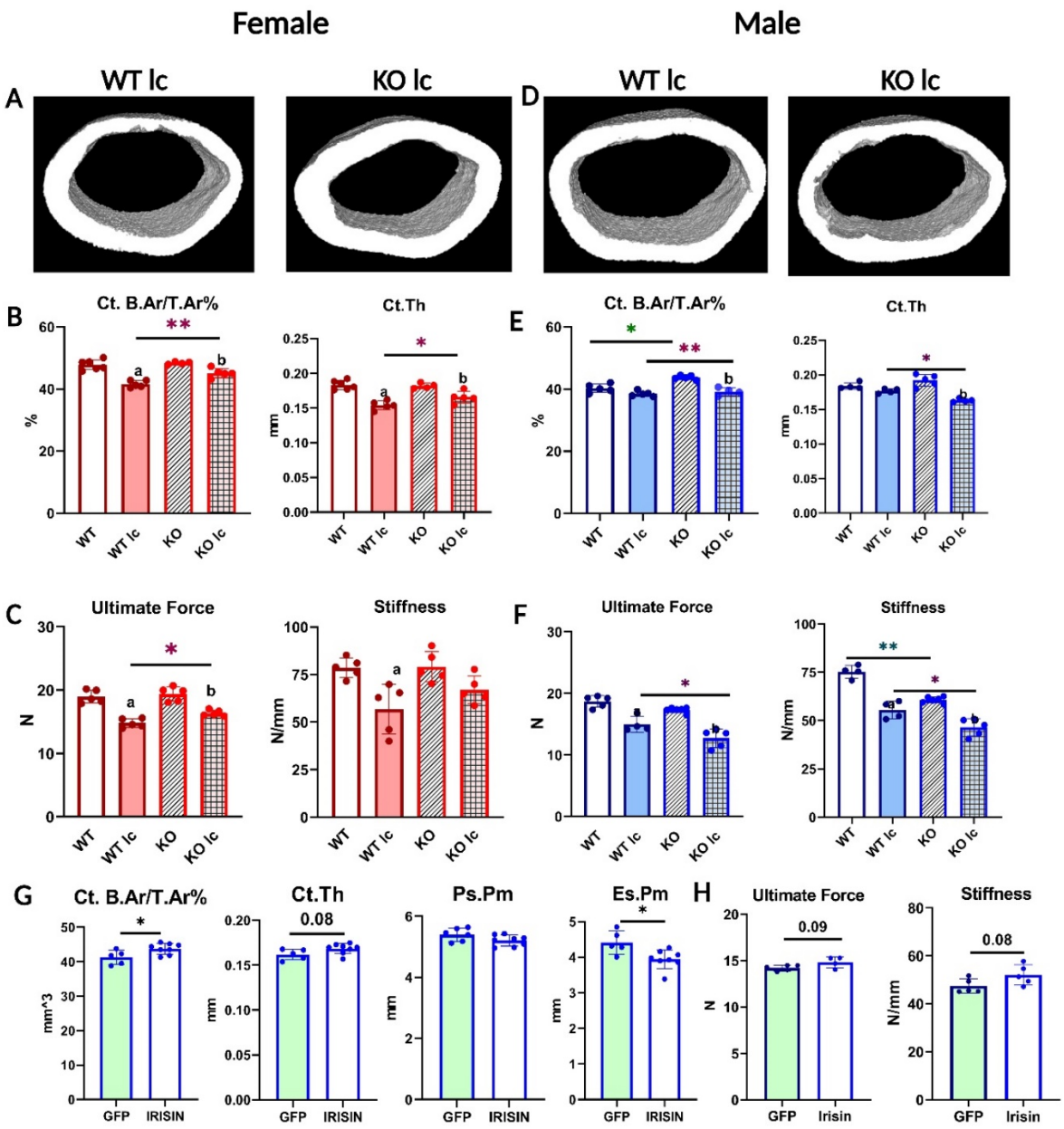

Fig 2: FNDC5 KO female and male mice have opposite responses to a low- calcium diet with regard to bone composition, structure, and mechanics, and irisin injection rescues FNDC5 KO male mice phenotype under a low- calcium diet

A: Representative µCT images of femoral midshaft cortical bones from WT low- calcium diet female mouse (WT lc) and KO low-calcium diet female mouse (KO lc).

B: Female femoral midshaft cortical bone parameters of WT control (WT), WT low-calcium diet (WT lc), KO control (KO), and KO low-calcium diet (KO lc) mice reported as cortical bone area fraction (Ct. B.Ar/T.Ar%) and cortical thickness (Ct.Th).

C: Mechanical properties of femurs from female WT and KO control and low- calcium diet

343 reported as ultimate force and stiffness.

344 **D:** Representative µCT images of femoral midshaft cortical bones from WT low-calcium diet
345 male mice (WT lc) and KO low-calcium diet male mice (KO lc).

346 **E:** Male femoral midshaft cortical bone parameters of WT control (WT), WT low-calcium diet
347 (WT lc), KO control (KO), and KO low-calcium diet (KO lc) mice reported as cortical bone area fraction
348 (Ct. B.Ar/T.Ar%) and cortical thickness (Ct. Th).

349 **F:** Mechanical properties of femurs from male WT and KO control and low- calcium diet
350 reported as ultimate force and stiffness.

351 n= 4-5/group. a= Significantly different from WT, b= Significantly different from KO, *= p<
352 0.05, **= p< 0.01. 2-way ANOVA with Tukey's post hoc test. As depicted here, red is female, and blue
353 is male.

354 **G:** µCT measurement of femoral cortical bone of AAV8-GFP or AAV8-irisin injected male KO
355 mice after a 2-week low calcium diet, reported as cortical bone area fraction (Ct. B.Ar/T.Ar%), cortical
356 thickness (Ct. Th), periosteal parameter (Ps.Pm), and endosteal parameter (Es.Pm).

357 **H.** Mechanical properties of femurs from male KO low-calcium diet mice injected with AAV8-
358 GFP or AAV8-irisin reported as ultimate force and stiffness.

359 n= 5-7/group, *= p< 0.05. Student's t-test was performed for statistical analysis between
360 male KO GFP vs irisin-injected mice. As depicted here, green shaded bars represent GFP-injected mice.

361

362 **Osteocytes from female and male KO mice respond differently to a low-**
363 **calcium diet**

364 To investigate if the bone loss was due to osteoclast or osteocyte
365 activation, tibiae from all the groups were TRAP-stained. Under a normal control
366 diet, the tibia from both KO female and male (Fig. 3A) mice had fewer TRAP-
367 positive osteocytes compared to their WT counterparts. This indicates that their
368 osteocytes were less 'primed' or 'activated' for resorption.

369 Under a low calcium diet, the number of TRAP-positive osteocytes increased
370 in both WT and KO female mice, similar to lactation (Fig 3A, Table 1), however, the
371 total number was still significantly lower in the KO females than the WT females.
372 The low calcium diet increased TRAP-positive osteocytes in both WT and KO male
373 mice. The KO male mice had a significantly higher level of increase (Fig 3A, Table
374 1), and had significantly higher TRAP-positive osteocytes compared to WT. This
375 indicates an increased activation of osteocytes in the KO males and suggests
376 higher osteocytic bone resorption.

There was no significant difference between WT and KO mice in osteoclast numbers per bone perimeter for both females and males (Fig. 3B). Both WT and KO females had an increase in their multinucleated TRAP-positive osteoclast number with a low-calcium diet, however, KO females had a significantly lower number of osteoclasts compared to WT females on a low-calcium-diet (Fig 3B). Similarly, under a normal diet, there was no difference in the number of osteo- clasts between male WT and KO. Under a low-calcium diet, osteoclast numbers increased in both groups, however, there was no significant difference between WT and KO male mice (Fig. 3B). We also measured osteoblast numbers per bone perimeter. There was no difference in osteoblast numbers in either female or male normal or low-calcium diet mice groups (data not shown).

Under normal control diet conditions, female WT mice had significantly higher osteocyte lacunar area compared to WT males (Fig 3C, 3D). There was no significant difference between FNDC5 KO female and male mice with regards to osteocyte lacunar area. This indicates that under control conditions, female osteocytes have more resorptive activity. On a low calcium diet, all the groups have increased osteocyte lacunar area, indicating an increased level of osteocytic osteolysis (Fig 3E). However, in female KO mice, the average lacunar area is significantly less than in WT female mice, similar to what was observed with the lactation response. The male KO mice, on the other hand, have significantly larger lacunar areas compared to WT males on a low calcium diet, suggesting in- creased osteocytic osteolysis. Together this data shows that bones from female KO mice are more resistant to calcium-demanding conditions, but the deletion of FNDC5/irisin from males makes them more susceptible to bone loss under calcium-demanding conditions. This also shows that male and female KO mice respond completely differently to the challenge of calcium deficiency.

Serum RANKL levels increased in all the low calcium diet groups compared to control diet groups (Fig 3F). There was no significant difference between WT and KO female mice and between WT and KO male mice. Serum PTH was measured because decreases in serum calcium stimulate the parathyroid gland to release PTH to remove calcium from bone to maintain normal calcium levels ***Jahn et al*** (***2017***); ***Matikainen et al*** (***2021***). PTH levels significantly increased in WT females and WT and KO males when subjected to a low calcium diet compared to the control diet (Fig 3G), however, the KO female group did not have a statistically

412 significant increase in PTH levels. There was no significant difference in serum
413 calcium levels in any of the groups (8-10 mg/dL range for all groups), which
414 indicates that the elevated PTH is maintaining normal circulating calcium levels in
415 these mice (Fig 3H).

416 Since irisin is robustly produced in skeletal muscle, we wanted to determine
417 if the deletion of irisin affects muscle function, under either a normal or a low
418 calcium diet. *In vivo* and *ex vivo* muscle contractility functions were performed in
419 these mice. No difference was found between WT and KO mice on either a
420 normal or a low calcium diet (Supplementary Fig 1). This indicates deletion of
421 FNDC5 is not affecting muscle function and that bone resorption is releasing
422 sufficient calcium into the circulation to maintain calcium homeostasis and
423 supplying sufficient calcium for skeletal muscle function.

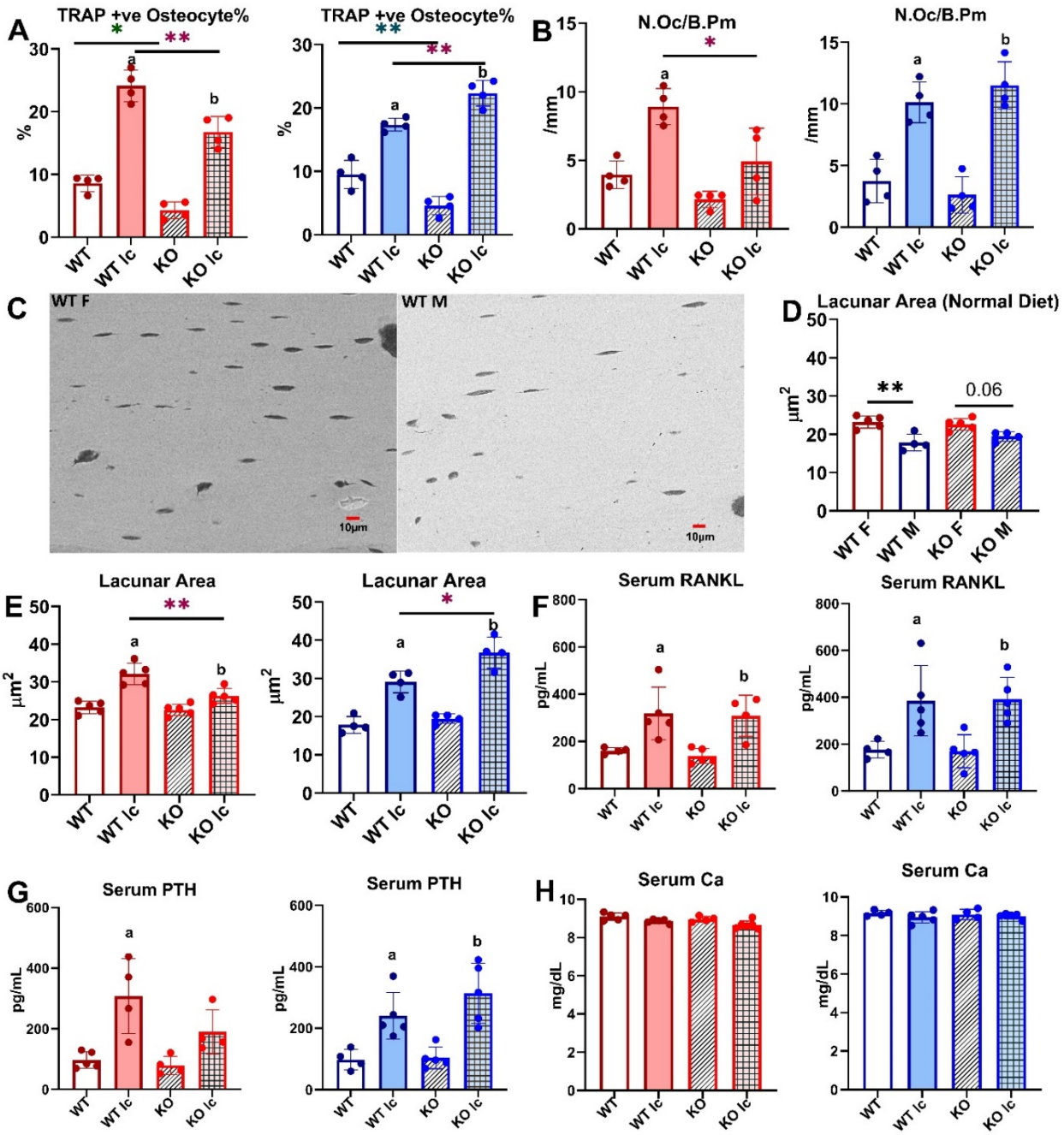

Fig 3: Osteocytes from female and male KO mice respond differently to a low-calcium diet

A: Percentage of TRAP-positive (+-ve) osteocytes in female and male WT and KO mice given a normal or a low-calcium diet.

B. Osteoclast number (N.Oc/B.Pm) in WT and KO female and male mice given a normal or a low-calcium diet.

C: Representative BSEM images depicting osteocyte lacunar area in femurs from WT female (WT F) and WT male (WT M) given a normal diet at 450X magnification.

433 **D.** Osteocyte lacunar area in WT and KO female and male mice given a normal diet

434 **E**: Lacunar area in female and male WT and KO mice given a normal or a low- calcium
435 diet.

436 **F:** Serum RANKL levels in female and male WT and KO mice given either a normal diet or
437 a low-calcium diet.

438 **G:** Serum PTH levels in female and male WT and KO mice given either a normal diet or a
439 low-calcium diet.

440 **H:** Serum calcium levels in female and male WT and KO mice given either a normal diet
441 or a low-calcium diet.

442 n= 4-5/group. a= Significantly different from WT, b= Significantly different from
443 KO, *= p< 0.05, **= p< 0.01. 2-way ANOVA with Tukey's post hoc test. As depicted here, red
444 is female, and blue is male.

445

Table 1: Bone Parameters and Serum Markers		% Change in female		% Change in male	
	Change	WT	KO	WT	KO
Bone Area	Decrease	13%	7% *	2%	13% *
Bone Area Fraction	Decrease	17%	11% *	7%	23% *
Cortical Thickness	Decrease	19%	13% *	4%	15% *
Osteoclast Number/Bone Perimeter	Increase	125%	127%	170%	336% *
TRAP-positive Osteocytes	Increase	180%	290% *	85%	388% *
Osteocyte Lacunar Area	Increase	38%	16% *	60%	89% *
Serum PTH	Increase	150%	75% *	70%	164% *
Serum RANKL	Increase	100%	118%	119%	130%

446

447 **Table 1: FNDC5 KO female and male mice have opposite responses to a low-calcium diet compared to**
448 **WT female and male mice where female KO mice are protected but male KO mice have greater bone loss**
449 **than WT.**

450 Percentage changes in different bone and serum parameters of WT and KO female and male mice with a
451 2-week low-calcium diet. *= p<0.05 compared to WT

452

453

454

455 **Female and male osteocyte transcriptomes are distinctly different**

456 Total RNA sequencing of osteocyte-enriched bone chips from female and male
457 WT mice revealed significant sex-dependent differences in the osteocyte
458 transcriptome under normal conditions (Fig. 4A, C, F). The major differentially
459 expressed genes were involved in the steroid, fatty acid, cholesterol, lipid
460 transport, and metabolic processes. Compared to male WT mice, female WT mice
461 had an approximately 2-3-fold higher expression of very low-density lipoprotein
462 receptor (*Vldlr*), voltage-dependent calcium channel T type alpha 1H subunit
463 (*Cacna1h*), aldehyde dehydrogenase (*Aldh1l2*), and a 2-3-fold lower expression of
464 apolipoproteins *Apoa1*, *Apoa2*, *Apoa4*, *Apoc3* and others involved in steroid and
465 fatty acid metabolic process. There was also a 2-3-fold lower expression of several
466 lipid and solute carrier genes and apolipoprotein genes in female WT compared
467 to male WT. This suggests that male osteocytes may be greater regulators and
468 utilizers of these sources of energy than female osteocytes.

469 Differences were also observed in genes involved in extracellular matrix
470 organization pathways, bone development, ossification, bone remodeling, and
471 re- sorption pathways. Female WT osteocytes have higher expression of genes
472 shown to be highly expressed in osteocytes during lactation compared to male
473 WT osteocytes. These include *Tnfsf11* (RANKL, 2.7-fold), *Ctsk* (2.5-fold), *Acp5*
474 (TRAP, 2.2- fold), *Mmp13* (2.7-fold), osteoclast associated receptor (*Oscar*, 4.6-
475 fold), macrophage stimulating 1 receptor (*Mst1r*, 3-fold), as well as several
476 collagen genes and bone formation and mineralization genes including alkaline
477 phosphatase (*Alpl*, 2.4-fold), periostin (*Postn*, 2.6-fold), and *Dmp1* (2.2-fold).
478 This suggests that the higher expression of bone formation genes may be to
479 accommodate the rapid replacement of the perilacunar matrix with weaning.
480 The upregulated and downregulated pathways in WT females compared to WT
481 males are depicted in Fig. 4.

482 **Female and male KO osteocyte transcriptomes have fewer differences**
483 **compared to WT female and male transcriptomes**

484 KO female and KO male osteocyte transcriptomes significantly
485 differed in pathways facilitating ossification and bone mineralization, and
486 extracellular structure and matrix organization (Fig. 4B, F). In KO females,
487 several collagen genes such as *Col2a1*, *Col5a2*, *Col8a2*, and *Col11a1* were 2-4-
488 fold greater compared to KO males. Bone formation genes including *Alpl* (2.5-
489 fold), osteocalcin (*Bglap*, 2.7-fold), *Postn* (2.9-fold), and *Wnt4* (2.4-fold) were

490 also more highly expressed in KO females compared to KO males, however,
491 the resorption genes including *Acp5* and *Ctsk* are not significantly different
492 between KO female and KO male osteocytes.

493 The transcriptomes of WT and KO male osteocytes differed significantly, with
494 much lower expression of genes in pathways involving steroid, fatty acid, lipid,
495 and cholesterol transport and metabolic processes in the KO males compared to
496 WT males (Fig. 4C, F). A 2-4-fold downregulation of genes coding for solute
497 carriers, aldehyde oxidase, and fatty acid binding proteins was observed in KO
498 males, while *Oscar* and *Mst1r* are 2-3-fold higher in KO males compared to WT
499 males. In contrast, a relatively low number of genes, 40, were differentially
500 expressed between WT female and KO female osteocytes which reflects the lack
501 of differences in bone morphology and bone mechanical properties (Fig. 4D, F).
502

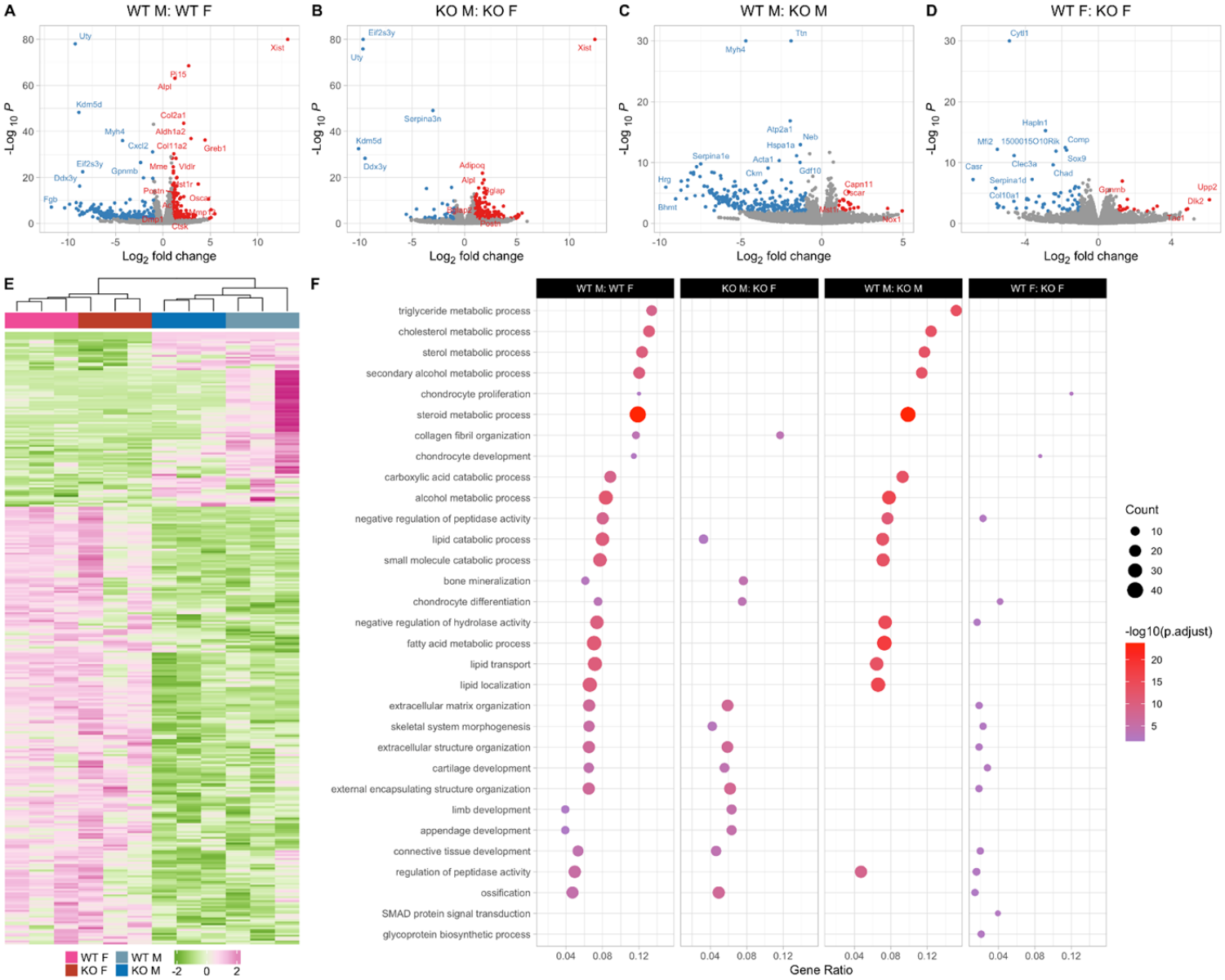

Fig 4: Female and male wildtype osteocyte transcriptomes are distinctly different; however, female and male KO osteocyte transcriptomes have fewer differences compared to WT female and male transcriptomes.

A: Volcano plot showing the significantly regulated genes between WT female control (WT F) and WT male control (WT M) osteocyte transcriptome

B: Volcano plot showing the significantly regulated genes between KO female control (KO F) and KO male control (KO M) osteocyte transcriptome

C: Volcano plot showing the significantly regulated genes between WT male control (WT M) and KO male control (KO M) osteocyte transcriptome

D: Volcano plot showing the significantly regulated genes between WT female control (WT F) and

515 KO female control (KO F) osteocyte transcriptome

516 **E**: Heat map showing the differentially expressed genes among WT female control (WT F), WT
517 male control (WT M), KO female control (KO F), and KO male control (KO M) osteocyte
518 transcriptome

519 **F**: Gene set enrichment analysis of Gene Ontology (GO) analysis of the significantly
520 regulated genes between WT female control (WT F) and WT male control (WT M) osteocyte
521 transcriptome, between KO female control (KO F) and KO male control (KO M) osteocyte
522 transcriptome, WT male control (WT M) and KO male control (KO M) osteocyte
523 transcriptome, and WT female control (WT F) and KO female control (KO F) osteocyte
524 transcriptome. The figure shows the union of the top 10 GO terms of each analysis. If a
525 term in the union, besides the top 10, is also significant (adjusted p-value less than 0.05) in
526 an analysis, it is also included in the figure. n=3/group

527

528 **With calcium deficiency, genes responsible for osteocytic osteolysis are**
529 **lower in the female KO compared to the female WT osteocyte**
530 **transcriptome**

531 Calcium deficiency in WT female mice induced higher expression of
532 osteoclast and resorption genes compared to WT females on a normal diet (Fig.
533 5A, E). *Acp5*, *Ctsk*, *Pth1r*, and *Mst1r* were elevated 2-4-fold in the calcium-deficient
534 WT females. Real-time PCR analysis of osteocytes also showed an increase in
535 *Tnsfs11*, *Acp5*, and *Ctsk gene* expression levels in the calcium-deficient WT
536 females compared to WT females on a normal diet. There was no difference in
537 *Sost* expression (Supplementary Fig 2D). Additionally, 5 different Mmps (*Mmp13*,
538 *Mmp15*, *Mmp2*, *Mmp16*, and *Mmp14*) were upregulated 2-3.5-fold in the WT
539 calcium-deficient females. These are genes thought to play a role in osteocytic
540 osteolysis. Bone formation and remodeling genes including *Bglap*, *Bglap2*, *Alpl*,
541 *Wnt 5a*, and *Wnt 2b* were upregulated 2-5-fold in the WT low calcium diet group
542 compared to WT female normal diet group as well. These genes may be increased
543 to provide quick bone formation upon return to normal calcium demand.

544 Calcium deficiency in KO female mice also induced increased expression of a
545 number of osteoclast and resorption genes including *Ctsk* (2.8-fold), *Mmp13* (3-
546 fold), and *Oscar* (2.6-fold) in comparison to KO female osteocytes on a normal diet
547 (Fig. 5B, E). However, unlike the WT osteocytes, expression of *Acp5* and *Pth1r* was
548 not different in osteocytes from KO female mice on a normal diet or a low

549 calcium diet. Real-time PCR analysis also showed an increase in *Ctsk* gene ex-
550 pression level in the calcium-deficient KO females compared to KO females on a
551 normal diet, with no significant difference in the expression levels of *Tnfsf11*, *Acp5*,
552 and *Sost* genes (Supplementary fig 2D).

553 Next, we compared KO female mice on a low-calcium diet to WT female mice
554 on a low-calcium diet (Fig. 5C, E). Several bone resorption genes were lower by
555 2-fold in KO females, including *Tnsfs11 and Mmp15*. Real-time PCR analysis also
556 showed a significantly lower expression of the *Tnsfs11* gene in the calcium-
557 deficient KO females compared to calcium-deficient WT females (Supplementary
558 Fig 2D). Additionally, bone formation genes including *Alpl*, *Bglap*, *Wnt2b*, *Col1a1*,
559 *Col1a2*, and *Postn* were also approximately 2-fold lower in the KO low calcium
560 females compared to WT low calcium females. This suggests that female KO
561 osteocytes are less responsive to calcium deficiency than female WT osteocytes.

Fig 5: The Osteocyte transcriptomes from female WT and KO mice are distinct when challenged with a low-calcium diet.

A: Volcano plot showing the significantly regulated genes between WT female control (WT C) and WT female low-calcium diet-fed mice (WT lc) osteocyte transcriptome

B: Volcano plot showing the significantly regulated genes between KO female control (KO C) and KO female low-calcium diet-fed mice (KO lc) osteocyte transcriptome

C: Volcano plot showing the significantly regulated genes between WT female low-calcium diet-fed mice (WT lc) and KO female low-calcium diet-fed mice (KO lc) osteocyte transcriptome

D: Heat map showing the differentially expressed genes among WT female control (WT C), WT female low-calcium diet-fed mice (WT lc), KO female control (KO C), and KO female low-calcium diet-fed mice (KO lc) osteocyte transcriptome

575 **E:** Gene set enrichment analysis of Gene Ontology (GO) analysis of the significantly
576 regulated genes between WT female control (WT C) and WT female low-calcium diet-
577 fed mice (WT lc) osteocyte transcriptome, between KO female control (KO C) and KO
578 female low-calcium diet-fed mice (KO lc) osteocyte transcriptome, and WT female low-
579 calcium diet-fed mice (WT lc) and KO female low- calcium diet-fed mice (KO lc)
580 osteocyte transcriptome. The figure shows the union of the top 10 GO terms of each
581 analysis. If a term in the union, besides the top 10, is also significant (adjusted p-value
582 less than 0.05) in an analysis, it is also included in the figure. n=2-3/group
583

584 **With calcium deficiency, genes responsible for bone resorption, bone for-**
585 **mation, and lipid metabolism are differentially regulated in the osteocyte**
586 **transcriptome in male KO mice compared to male WT mice.**

587 Calcium deficiency in WT male mice caused a 2-7-fold increased expression of
588 *Tnsfs11*, *Acp5*, *Ctsk*, *Oscar*, and *Mst1r* in their osteocyte transcriptome compared
589 to WT males on a normal diet (Fig. 6A, E). Real-time PCR validation also showed
590 a similar increase in *Tnsfs11*, *Acp5*, and *Ctsk* gene expression levels in the calcium-
591 deficient WT males compared to WT males on a normal diet (Supplementary Fig
592 2E). Bone formation and remodeling genes including *Postn*, *Col1a1*, *Col1a2*, *Bglap*,
593 and *Wnt4* were also elevated 2-4-fold in the WT male low calcium diet compared
594 to the WT normal diet control group.

595 Multiple genes involved in the steroid and fatty acid metabolic process
596 pathways as well as lipid catabolic processes were downregulated 2-7-fold in the
597 calcium-deficient WT males compared to WT males on a normal diet. These genes
598 include several solute carrier family protein genes *Slc27a2* and *Slc27a5*, several
599 apolipoprotein genes including *Apoa1*, *ApoB*, and *Apoc1*, several cyp genes
600 including *Cyp2e1* and *Cyp7a1*, and *Plin1*.

601 Similarly, osteocytes from KO males on a low calcium diet had a 2-4-fold higher
602 expression of osteoclast genes such as *Tnsfs11*, *Oscar*, and *Car3* and a 2-5-fold up-
603 regulation of bone formation genes such as *Col1a1*, *Col1a2*, *Alpl*, *Bglap*, and *Postn*
604 compared to osteocytes from KO males on a normal diet (Fig. 6B, E). Therefore,
605 genes responsible for bone resorption and bone formation are increased in both
606 WT and KO with calcium deficiency. Real-time PCR data showed an increase in
607 *Tnsfs11*, Acp5, and *Ctsk* gene expression levels in the calcium-deficient KO males
608 compared to KO males on a normal diet, validating the RNA sequencing data
609 (Supplementary Fig 2E).

When KO males were compared to WT males on a low calcium diet (Fig. 6C, E), there was a 2-3-fold higher expression of bone resorption genes including *Oscar* and *Mst1r* in the KO low calcium diet males compared to WTs. Several collagen formation genes and ossification genes including *Col3a1*, *Col8a2*, *Tnn*, *Aspn*, and *Igfbp6* were also significantly downregulated in the KO males on a low-calcium diet compared to WTs on a low-calcium diet. It is not clear whether these also play a role in the increased bone resorption observed with calcium deficiency in KO males. Real-time PCR analysis showed no significant difference in expression levels of *Tnsfs11*, *Acp5*, *Sost*, and *Ctsk* genes between calcium-deficient KO males and calcium-deficient WT males, reflecting the RNA sequencing data (Supplementary Fig 2E). No significant difference was observed in expression levels of genes involved in the lipid catabolic process pathway or fatty acid metabolism pathways.

Fig 6: The Osteocyte transcriptomes from male WT and KO mice are dis- tinct when challenged with a low-calcium diet.

A: Volcano plot showing the significantly regulated genes between WT male control (WT C) and WT male low-calcium diet-fed mice (WT lc) osteocyte transcriptome

B: Volcano plot showing the significantly regulated genes between KO male control (KO C) and KO male low-calcium diet-fed mice (KO lc) osteocyte transcriptome

C: Volcano plot showing the significantly regulated genes between WT male low-calcium diet-fed mice (WT lc) and KO male low-calcium diet-fed mice (KO lc) osteocyte transcriptome

D: Heat map showing the differentially expressed genes among WT male control (WT C), WT male low-calcium diet-fed mice (WT lc), KO female control (KO C), and KO male low-calcium diet-fed mice (KO lc) osteocyte transcriptome

E: Gene set enrichment analysis of Gene Ontology (GO) analysis of the significantly regulated genes between WT male control (WT C) and WT male low- calcium diet-fed mice (WT lc) osteocyte transcriptome, between KO male control (KO C) and KO male low-calcium diet-fed mice (KO lc) osteocyte transcriptome, and WT male low-calcium diet-fed mice (WT lc) and KO male low-calcium diet-fed mice (KO lc) osteocyte transcriptome. The figure shows the union of the top 10 GO terms of each analysis. If a term in the union, besides the top 10, is also significant (adjusted p-value less than 0.05) in an analysis, it is also included in the figure.

n=3/group

Discussion

Irisin has been shown to be increased in the blood of humans and mice with exercise. Irisin, working mainly through its receptor $\alpha V\beta 5$ integrin, has been shown to have powerful effects on fat, bone, and brain tissues ***Bostrom et al.*** (***2012***); ***Tsourdi et al.*** (***2022***); ***Korta et al.*** (***2019***); ***Islam et al.*** (***2021***); ***Kim et al.*** (***2018***); ***Colaianni et al.*** (***2017***); ***Wrann et al.*** (***2013***); ***Xin et al*** (***2016***); ***Wang et al.*** (***2017***); ***Bao et al.*** (***2022***); ***Zhang et al.*** (***2022***). With regard to bone, studies have generated complex and even contradictory results ***Erickson*** (***2013***); ***Maak et al.*** (***2021***); ***Colaianni and Grano*** (***2015***); ***Kim et al.*** (***2018***); ***Estell et al.*** (***2020***);

656 *Colaianni et al.* (*2014*); *Zhang et al.* (*2018*). Of note, the majority of bone studies
657 have been performed either exclusively on males, or females, but few on both.
658 Most studies have used recombinant irisin treatment whereas we have focused on
659 the effects of deleting irisin. Other studies have mainly examined the effects on
660 osteoblasts and osteoclasts, whereas our studies have focused on osteocytes *Kim*
661 *et al.* (*2018*).

662 Global deletion of FNDC5 had essentially no effect on bone in females, but in
663 contrast, the null male mice have significantly more bone compared to wildtype
664 males, but this bone has impaired mechanical properties. This suggests that the
665 lack of FNDC5 is having no effect on the development or growth of the female
666 skeleton, but does affect the male skeleton, increasing the size yet impairing
667 matrix properties responsible for strength. Examination of their osteocytes
668 showed that both female and male null mice have significantly fewer TRAP-
669 positive osteocytes compared to their sex-matched wildtype controls
670 suggesting that their osteocytes are more quiescent or less primed for bone
671 resorption.

672 Challenging the null animals with calcium deficiency revealed dramatic
673 differences in osteocytic osteolysis and osteoclast activation, two major
674 functions of osteocytes. Deletion of FNDC5 in females is partially protective
675 against calcium deficiency, but deletion in males accelerates both of these
676 osteocyte functions resulting in greater bone loss compared to controls. We
677 have shown previously that under calcium-demanding conditions such as
678 lactation, osteocytes express genes previously thought only to be specific for
679 osteoclasts including cathepsin K, TRAP, carbonic anhydrase, the proton pump V-
680 ATPase, and others *Qing et al.* (*2012*) and shown that osteocytes are the major
681 source of RANKL *Nakashima et al.* (*2011*); *Xiong and O'Brien* (*2012*); *Xiong et*
682 *al.* (*2015*). In this study, lactating females lacking FNDC5 were partially resistant
683 to bone loss, similar to ovariectomized females as previously published *Kim et al.*
684 (*2018*). To determine the effects of calcium deficiency on males, mice were given
685 a low-calcium diet for 2 weeks. Unlike the protective effects of FNDC5/irisin
686 deletion in females, bone loss was exacerbated in null males compared to
687 controls on a low calcium diet.

688 With two weeks of lactation and litter size comparable to wildtype controls,
689 the null female mice had less circulating RANKL, fewer TRAP-positive osteoclasts,
690 fewer TRAP-positive osteocytes, and smaller lacunar size. Our observation that

691 the deletion of FNDC5/ irisin makes lactating mice partially resistant to bone loss
692 has an important implication with regard to the purpose of lactation. Lactation
693 is a critical period for pups as they obtain essential nutrients, especially calcium,
694 from the mother's milk for their proper growth. Calcium lost by the mother's
695 bone during lactation is rapidly replaced upon weaning with complete recovery
696 of bone mass within a week ***Qing et al.*** (***2012***); ***Wysolmerski*** (***2002***); ***Kalkwarf***
697 (***2004***); ***Kovacs*** (***2001***); ***Wysolmerski*** (***2012***). Our data suggest that irisin acts as a
698 regulator of calcium release from maternal bones to fulfill the offspring demands
699 during lactation. Therefore, irisin appears to play a beneficial role in ensuring
700 offspring survival and consequently, successful reproduction.

701 To determine if low calcium would have a similar effect on male FNDC5 null
702 bone, both males and females were subjected to a low-calcium diet for 2 weeks.
703 The effects of a low-calcium diet on female osteocytes and bone loss were
704 essentially identical to the effects of lactation, with two exceptions. First, serum
705 RANKL levels were not significantly different between virgin and lactating null
706 females, while they were between null females on a normal compared to a
707 calcium diet suggesting that RANKL plays less of a role in lactation compared to
708 calcium deficiency. Secondly, the medullary cavity and endosteal bone in the low-
709 calcium females were completely protected in the FNDC5 null females but were
710 not in the lactating FNDC5 null mice. Bone loss due to lactation or due to dietary
711 calcium deficiency may target different bone sites. Our unpublished observations
712 suggest that endosteal bone is removed faster than periosteal bone with lactation,
713 but this remains to be carefully validated. This difference may also be due to
714 elevated PTHrP during lactation ***Kovacs*** (***2001***), whereas hypocalcemia increases
715 circulating PTH levels ***Goltzman*** (***2008***), and it is not clear if hormones target
716 distinct bone sites. Similar to the lactating FNDC5 null mice, the null females
717 placed on the low calcium diet had fewer TRAP-positive osteoclasts, fewer TRAP-
718 positive osteocytes, and smaller lacunar size. Serum RANKL levels increased in
719 both wildtype and null mice with dietary calcium deficiency, therefore, serum
720 RANKL alone is not enough to explain the partial protective effect of FNDC5
721 deletion against bone loss. In summary, female null mice are not only resistant
722 to bone loss due to estrogen deficiency as we showed previously ***Kim*** (***2018***) but
723 are also resistant to calcium deficiency either due to an increase in PTHrP as
724 with lactation, or an increase in PTH as with a low calcium diet.

725 Osteoporosis manifests earlier in females due to menopause, but males also

726 develop osteoporosis but at an older age ***Johannesdottir et al.*** (***2013***);
727 ***Johnston and Dagar*** (***2020***), and the elderly are known to suffer from calcium
728 deficiency which accelerates bone loss ***Kumssa et al.*** (***2015***); ***Body et al.***
729 (***2016***). Dietary calcium deficiency has been shown previously to affect female
730 and male bone differently where female rat bones are more sensitive to a low
731 calcium diet compared to males ***Geng and Wright*** (***2001***). Similarly, in our
732 study, we saw that wildtype females were more affected by calcium deficiency
733 and lost more bone compared to wildtype male mice. However, the opposite
734 was observed for the FNDC5/irisin null mice, where female null mice were
735 partially resistant, and male null mice were more susceptible to bone loss with
736 calcium deficiency compared to their wildtype counterparts. Despite starting
737 with more bone volume compared to wildtype, the FNDC5 null males had
738 increased osteocyte lacunar area and lost more bone with dietary calcium
739 deficiency compared to wild-type males. This greater bone loss can be
740 explained through the dramatic increase of TRAP-positive osteocytes and TRAP-
741 positive osteoclasts, but not by a significantly greater increase in circulating
742 RANKL. This sex difference indicates that FNDC5/irisin may be involved in the
743 regulation of calcium release from bone via osteocytes in a sex-dependent
744 manner.

745 Lacunar area is an indicator of osteocyte regulation of their lacunar
746 microenvironment. Here we report that osteocyte lacunar size is significantly
747 larger in virgin wildtype female mice compared to same-age wildtype males. This
748 difference in lacunar area indicates a distinction between female and male
749 osteocyte function. The mammalian skeleton is a sexually dimorphic organ
750 ***Sharma*** (***2023***), and female and male bones respond differently to circulating
751 factors, hormones, and myokines as well as other challenges ***Kurapaty and Hsu***
752 (***2022***); ***Lu et al.*** (***2022***); ***Osipov et al.*** (***2022***). As osteocytes are regulators of bone
753 formation and resorption ***Bonewald*** (***2011***); ***Dallas et al.*** (***2013***); ***Robling and***
754 ***Bonewald*** (***2020***), this sex difference may be due to differences in male and
755 female osteocytes. A recent study by Youlten and colleagues has shown that
756 male and female osteocyte transcriptomes are distinctly different ***Youlten et***
757 ***al.*** (***2021***). At 4 weeks of age, the female osteocyte transcriptome diverges
758 from the male osteocyte transcriptome and these differences continue with
759 age. A cluster of genes more highly expressed in female osteocytes compared
760 to male osteocytes are those involved in bone resorption, the same ones

761 elevated in osteocytes in response to lactation. These transcripts include genes
762 necessary for osteocytic perilacunar remodeling and reduction in pH, which are
763 essential for calcium removal ***Qing et al.*** (***2012***). This suggests that the larger
764 lacunar area in female osteocytes compared to male osteocytes may be due to
765 the higher expression of bone resorption genes.

766 To begin to understand the molecular mechanisms responsible for the sex
767 and genotype differences, we compared the osteocyte transcriptomes of 5-month-
768 old female and male, wildtype and null mice. Our results show that the
769 osteocyte transcriptomes of female and male wildtype mice are significantly
770 different under normal conditions. A surprising difference not described in the
771 Youlten paper ***Youlten et al.*** (***2021***) was that compared to wildtype female
772 osteocytes, wildtype male osteocytes have much higher expression of genes
773 involved in steroid, lipid, and cholesterol metabolism and transport pathways,
774 lipid and solute carrier genes, and apolipoprotein genes. This suggests that
775 osteocyte metabolism and bioenergetics are distinctly different between
776 wildtype females and wildtype males. We hypothesize that the differentially
777 expressed genes in these bioenergetic and metabolic pathways modulate bone
778 mass and formation and may shed light on the sexual dimorphism of bones. As
779 these differentially regulated path- ways were not previously reported by
780 Youlten ***Youlten et al.*** (***2021***), this may be due to differences in strain, housing,
781 diet, or microbiome. Another explanation is the greater osteocyte purity in our
782 study as we used a series of collagenase digestions and EDTA chelation to remove
783 any surface cells which was not performed in the Youlten paper ***Youlten et al.***
784 (***2021***).

785 A second major difference between female and male wildtype osteocytes was
786 the higher expression of genes involved in collagen matrix formation, bone
787 mineralization, remodeling, resorption, and osteocytic osteolysis pathways in
788 females compared to males. Many of the highly expressed bone resorption
789 genes in wild- type female osteocytes have been shown to be elevated during
790 lactation ***Qing et al.*** (***2012***) including *Acp5*, *Ctsk*, and *Mmp13*, all involved in
791 osteocytic osteolysis. This further supports our hypothesis that wildtype female
792 osteocytes are more primed for resorption compared to wildtype males,
793 presumably to meet the increased calcium demand during lactation, and
794 correlates with the observed larger lacunae compared to males.

795 Few differences were observed between wildtype female and null female

796 osteocyte transcriptomes as would be expected as the only difference
797 observed was the number of TRAP-positive osteocytes. In contrast, osteocytes
798 from wild- type males and null males are significantly different with regards to
799 fatty acid and lipid metabolism pathways where null male mice have lower
800 expression of these genes compared to wildtype males. This suggests a role for
801 irisin in lipid metabolism and bioenergetics in male osteocytes. Lower
802 expression in the null male mice may be responsible for the higher bone mass
803 and inferior biomechanical properties compared to wildtype males suggesting
804 these pathways mediate the effects of irisin on male bone.

805 Osteocytes from null females have higher expression of genes and pathways
806 involved in collagen matrix organization, ossification, and mineralization
807 compared to null males. Unlike wildtype males and females, there was no
808 difference in expression of lipid, cholesterol, and fatty acid metabolism genes in
809 null males compared to null females. Again, this indicates that irisin regulates
810 male bone through these lipid-related pathways.

811 Lactation and calcium deficiency induce the same changes in females. Similar
812 to that reported previously for lactation ***Qing et al.*** (***2012***), osteocytes from wild-
813 type female mice on a low calcium diet exhibited an increase of several osteo-
814 clast/resorption/lactation genes including *Acp5*, *Ctsk*, *Oscar*, *Mst1r*, and *Pth1r* com-
815 pared to wildtype females on a normal diet. Surprisingly, we also observed an
816 increase in bone formation genes including *Col1a1*, *Alpl*, and *Bglap*. As osteocytic
817 osteolysis is rapidly reversed within a week of weaning, the osteocyte may be
818 preparing to rapidly reverse bone loss. We propose that once calcium is re-
819 plenished, shutting off the proton pump will rapidly reverse the pH within the
820 osteocyte lacunae, allowing bone-forming proteins such as alkaline phosphatase
821 to become active to rapidly replace the osteocyte perilacunar matrix ***Jahn et al.***
822 (***2017***); ***Andersson et al.*** (***2003***); ***Silver et al.*** (***1988***); ***Kaplan*** (***1972***); ***Farley and***
823 ***Baylink*** (***1986***).

824 The main molecular mechanism responsible for the resistance of null female
825 mice to calcium deficiency compared to wildtype female mice is lower expression
826 of genes such as *Tnfsf11*, responsible for osteoclastic resorption. A
827 correspondingly lower expression of bone formation genes including *Col1a1*,
828 *Alpl*, and *Bglap* compared to wildtype females on a low-calcium diet was
829 observed. The lower expression of both formation and resorption genes
830 suggests a coupling of re- sorption with formation. Irisin appears to regulate

calcium release in the female skeleton.

Osteocytes from wildtype male mice on a low calcium diet expressed higher levels of bone resorption genes including *Tnsfs11*, *Acp5*, *Ctsk*, *Oscar*, and *Mst1r* compared to wildtype male mice on a normal diet as expected. Like the females, there is a coupling with bone formation genes as there is also an increase in *Bglap* and *Col1a1*, suggesting the potential for osteocytes to rapidly replace their peri-lacunar matrix with calcium repletion. Similarly, the male null mice with calcium deficiency showed an increase in bone resorption genes including *Tnsfs11*, *Oscar*, and *Car3*, as well as an increase in bone formation genes such as *Alpl* and *Bglap* compared to null mice on a normal diet. The major differences between wild-type male mice with calcium deficiency and FNDC5-null male mice with calcium deficiency were the lower expression of genes involved in the extracellular matrix organization, ossification, and bone development pathways in the null male mice compared to wildtype males. This suggests a mechanism for how null male mice lose more bone with calcium deficiency compared to wildtype males.

Irisin could be having direct or indirect effects on osteocytes. Irisin can modulate adipose tissue ***Bostrom et al.*** (***2012***); ***Zhang et al.*** (***2014***); ***Celi and Brown*** (***2017***); ***Luo et al.*** (***2022***), can potentially modulate osteogenic differentiation of bone marrow mesenchymal stem cells through αVβ5 ***Zhu et al.*** (***2023***) and bone marrow adipose tissue can modulate bone properties ***Yeung et al.*** (***2005***); ***Rosen and Bouxsein*** (***2006***); ***Muruganandan and Sinal*** (***2014***); ***Styner et al.*** (***2015***); ***Schwartz et al.*** (***2015***); ***During*** (***2020***) as well as osteocyte number and activity ***Saedi A et al.*** (***2019***, 2020). Irisin can modulate brain activity and signaling ***Islam et al.*** (***2021***); ***Wrann et al.*** (***2013***); ***Young et al.*** (***2019***); ***Jo and Song*** (***2021***); ***Qi et al*** (***2022***) through BDNF ***Wrann et al.*** (***2013***) and BDNF promotes osteogenesis in human bone mesenchymal stem cells ***Liu et al.*** (***2018***). Potential indirect effects on osteocytes remain to be confirmed.

Irisin must bind to αVβ5 integrins to function. Osteocytes express high levels of this receptor which was first discovered using the female MLO-Y4 osteocyte- like cell line ***Kim et al.*** (***2018***). Integrins are usually stable in the cell membrane with a half-life of 12-24 hours ***Moreno-Layseca et al.*** (***2019***). In our RNA sequencing data, we observed a stable expression of both *ITGAV* and *ITGB5*, encoding integrins αV and β5 respectively, with no differences between either wildtype or null, male or female, calcium replete or calcium deficient mice. Recently it has

been published that Hsp90α is necessary to facilitate irisin-αVβ5 binding ***Mu et al.*** (***2023***). *Hsp90a*, the gene encoding this heat shock protein, is very highly expressed in both wild- type and null male and female mice, with no significant regulation by diet. The high expression of Hsp90α in osteocytes may explain their significant and rapid responses to irisin ***Kim et al*** (***2018***). Our data do not show significant expression of *Fndc5* in osteocytes.

In summary, FNDC5/irisin deletion has few if any effects on the female skeleton but a significant effect on the male skeleton resulting in more but weaker bone. However, with challenges, such as calcium deficiency, dramatic differences were observed. Our data suggest that irisin activates the osteocyte in females to initiate the removal of their perilacunar matrix and for bone resorption through osteoclast activation, presumably to provide calcium for reproduction purposes. In contrast, in males, irisin protects against osteocytic osteolysis and osteoclastic bone resorption under calcium-demanding conditions. This sex-specific effect may be due to the sexual dimorphism of the osteocyte transcriptome. We have discovered a new novel function of irisin to ensure the survival of offspring and that irisin is essential for male but not female skeletal development. These findings could have implications for understanding sex-dependent differences in bone diseases, such as osteoporosis, and lead to the development of sex- targeted therapies.

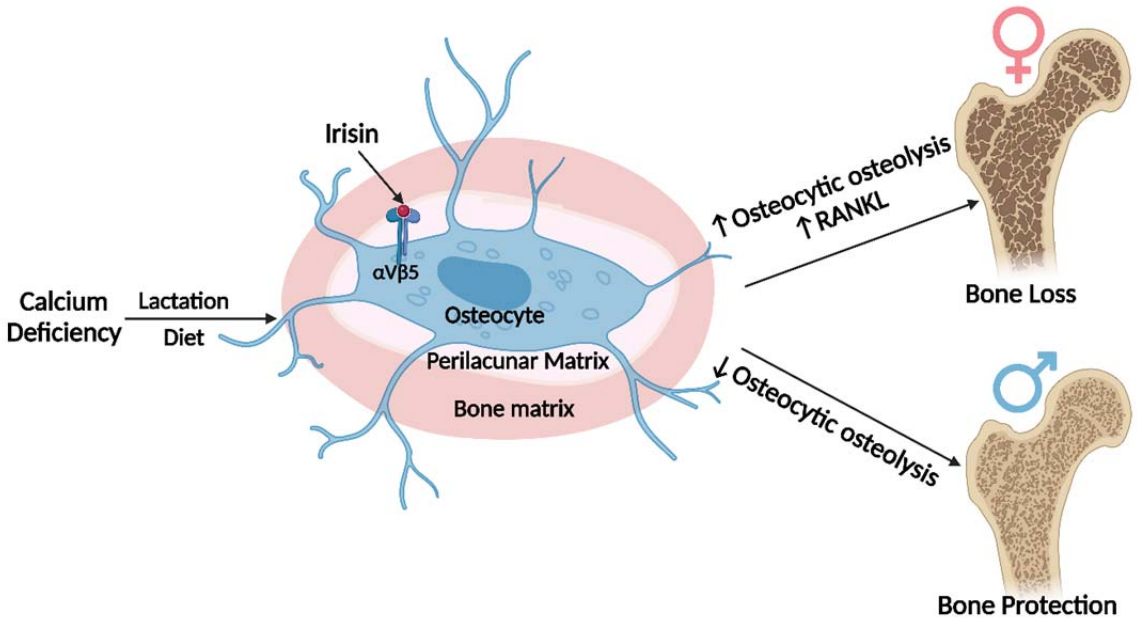

Fig 7: Graphical abstract (image was created using BioRender.com)

- No differences are observed in bone from Fndc5 /irisin null female, whereas null male skeletons are larger but weaker compared to wildtype controls.
- With calcium deficiency, lactating female null mice are protected from bone loss due to osteocytic osteolysis, whereas male null mice on a low calcium diet lose greater amounts of bone compared to their wildtype controls.
- The osteocyte transcriptomes show wildtype males have higher expression of the steroid, lipid and fatty acid pathways which are lower in the null males, whereas the wildtype females have higher expression of genes regulating osteocytic osteolysis than null females.
- With calcium deficiency, female null osteocytes have lower while male null osteocytes have higher expression of osteocytic osteolysis genes compared to wildtype controls.

Methods

Animal Experiments

All animal experiments were performed per procedures approved by the Institutional Animal Care and Use Committee (IACUC) of the Indiana University School of Medicine. Heterozygous C57Bl/6J FNDC5 Knockout (KO) mice were provided by Dr. Bruce Spiegelman at Harvard University and bred in our facility to obtain homozygous global FNDC5 KO and wildtype (WT) control mice. Genotype was determined using a PCR reaction with primers targeting portions of exon 3 absent in KO (WT Forward: GCG GCT CGA GAG ATG AAG AA, WT Reverse: CAG CCC ACA ACA AGA AGT GC, KO Forward: GGA CTT CAA GTC CAA GGT CA, KO Reverse: CCT AAG CCC ACC CAA ATT AC). Mice were housed in a temperature-controlled (20–22°C) room on a 12-hour light/dark cycle with ad libitum food and water. Qualified veterinary staff and/or animal care technicians performed regular health check inspections.

For the lactation experiments, 4-month-old WT and FNDC5 global KO female mice were bred, delivered pups, and lactated for 2 weeks before sacrifice. Virgin

921 WT and KO mice were used as controls. All animals were 4-5 months old at the
922 time of sacrifice and analysis. For all lactating mice, the litter size ranged from
923 8-11 pups ***Qing et al.*** (***2012***).

924 For the low calcium diet experiments, 4-5-month-old male and female WT and
925 FNDC5 global KO mice were fed either a control diet (0.6% calcium, Teklad,
926 TD.97191) or a low calcium (Ca) diet (0.01% calcium, 0.4% phosphorus, Teklad
927 TD.95027) for 2 weeks. Distilled water was used in place of tap water to control
928 calcium intake. On the day of sacrifice, blood was collected under anesthesia, and
929 mice were euthanized for sample collection, processing, and analysis ***Qing*** (***2012***);
930 ***Jahn et al.*** (***2017***).

931 **AAV8 injection**

932 AAV8-irisin and AAV8–GFP constructs were obtained from Dr. Bruce
933 Spiegelman at Harvard University. AAV8 Mouse ORF 1-140 (containing the N-
934 terminal signal peptide and irisin) plus a five-amino-acid linker plus a C-terminal
935 flag tag was cloned into the pENN.AAV.CB7.CI.pm20d1flag.WPRE.rBG vector
936 (Addgene plasmid no. 132682). AAV8-GFP (pENN.AAV.CB7.CI.eGFP.WPRE.rBG),
937 used as control, was obtained from Addgene (105542), and packaged at the
938 UPenn Vector Core to a titer of 2.10 × 1013 GC per ml39. FNDC5 KO male mice
939 were placed under anesthesia and injected into the tail vein with either AAV8-
940 irisin or AAV8-GFP control (1 X 10^{10} GC per mouse) in 100 μL in PBS ***Islam et al.***
941 (***2021***). One week after injection with either the control virus containing GFP or
942 the virus coding for circulating irisin, the mice were placed on a low-calcium diet
943 for two weeks before sacrifice.

944 ***In vivo* and *ex vivo* muscle contractility and electrophysiology**
945 **measurement**

946 *In vivo* plantarflexion torque was assessed one day before sacrifice (Scientific
947 Inc, Canada) as described in ***Pin et al.*** (***2022***). Briefly, the mouse was placed under
948 anesthesia and the left hind foot was affixed to the force transducer aligned with
949 the tibia at 90°. The tibial nerve was stimulated using monopolar electrodes
950 (Natus Neurology, Middleton, WI). Maximum twitch torque was established by
951 using a 0.2 ms square wave pulse. Peak plantarflexion torque was measured by
952 using a stimulation of 0.2 ms delivered at 100Hz stimulation frequency.

953 *In vivo* electrophysiological functions were assessed one day before sacrifice
954 with the Sierra Summit 3–12 Channel EMG (Cadwell Laboratories Incorporated,

955 Kennewick, WA, USA) as described in ***Huot et al.*** (***2022***). Briefly, peak-to-peak
956 and baseline-to-peak compound muscle action potentials (CMAP) were
957 measured using supramaximal stimulations of <10 mA continuous current for 0.1
958 ms duration, and peak-to-peak single motor unit (SMUP) potentials were
959 measured using an incremental stimulation technique. Motor unit number
960 estimation (MUNE) was measured using the equation: MUNE = CMAP
961 amplitude/average SMUP.

962 *Ex vivo* muscle contractility was measured in the extensor digitorum longus
963 (EDL) muscle as described in ***Huot et al.*** (***2021***). EDL was collected from the
964 mouse and mounted between a force transducer, and then submerged in a
965 stimulation bath. The muscles were forced to contract, and data were
966 collected using Dynamic Muscle Control/Data Acquisition (DMC) and Dynamic
967 Muscle Control Data Analysis (DMA) programs (Aurora Scientific). The EDLs were
968 weighed for normalization purposes.

969 **Body composition assessment by dual-energy X-ray absorptiometry (DXA)**

970 The right femurs from mice were dissected and cleaned of soft tissue, fixed in
971 4% paraformaldehyde (PFA) for 48 hours, and then transferred to 70% ethanol.
972 Ex vivo DXA measurements were obtained using a faxitron (Faxitron X-ray Corp,
973 Wheeling, IL) to measure bone mineral density (BMD) and bone mineral content
974 (BMC) ***Essex et al.*** (***2022***).

975 **Bone morphometry analysis by micro-computed tomography (μCT)**

976 Right femurs were analyzed using a Skyscan 1176 μCT as described
977 previously ***Pin et al.*** (***2022***). Briefly, specimens were scanned at 55 kV, 145 μA,
978 high resolution, 10.5 mm voxel, and 200 ms integration time. For cortical
979 parameters, three- dimensional images from a 1mm region of interest (ROI) of
980 the mid-diaphysis were used to calculate total cortical bone area fraction (Ct.
981 B.Ar/T.Ar%), cortical bone thickness (Ct. Th), marrow cavity area, periosteal
982 perimeter (Ps. Pm), and endosteal perimeter (Es. Pm) according to ASBMR
983 guidelines ***Bouxsein et al.*** (***2010***). For trabecular parameters, three-
984 dimensional images reconstructed within the range of 0.5 mm from the most
985 proximal metaphysis of tibiae were analyzed. Trabecular morphometry was
986 performed by excluding the cortical bone from the endocortical borders using
987 hand-drawn contours followed by thresholding and characterized by bone
988 volume fraction (BV/TV), trabecular number (Tb. N), trabecular thickness (Tb.
989 Th), trabecular spacing (Tb. Sp), and connectivity density (Conn.D) ***Kitase et al.***

990 (*2018*).

991 **Tartrate-resistant acid phosphatase (TRAP) staining**

992 Tibiae were stripped of soft tissue, fixed in 4% PFA for 48 hours, decalcified
993 in 10% EDTA for 3-4 weeks, and processed into paraffin as described
994 previously followed by sectioning (5 μm) and staining for TRAP activity using
995 the standard naphthol AS-BI phosphate post coupling method and counterstained
996 with toluidine blue *Pin et al.* (*2021*). Briefly, after equilibration in 0.2 M sodium
997 acetate, 50 mM sodium tartrate, pH 5.0, for 20 min at RT, sections were incubated
998 at 37°C in the same buffer containing 0.5 mg/ml naphthol AS-MX phosphate
999 (Sigma Chem. Co., St. Louis, MO) and 1.1 mg/ml Fast Red Violet LB salt (Sigma)
1000 and counter- stained in toluidine blue. Images were taken at 5X and 40X using an
1001 Olympus BX51 fluorescent microscope and Olympus cellSense Entry 1.2(Build
1002 7533) imaging software. TRAP-positive osteocytes and osteoclasts 1.5 mm distal
1003 from the growth plate were quantified using Osteomeasure software
1004 (OsteoMetrics.Inc) in a blinded fashion. Toluidine blue-stained osteoblasts from
1005 the same sections were quantified 1.5 mm distal from the growth plate using the
1006 same software.

1007 **Osteocyte lacunar area measurement by Backscatter Scanning Electron**
1008 **Microscopy (BSEM)**

1009 Femurs were stripped of soft tissue and fixed in 4% PFA for 48 hours before
1010 proceeding to dehydration and embedding steps as previously described
1011 *Qing et al.* (*2012*). Briefly, femurs were dehydrated in graded ethanol and
1012 placed into acetone. Subsequently, the femurs were immersed in infiltration
1013 solution made of 85% destabilized methyl methacrylate (MMA, Sigma), 15%
1014 dibutyl phthalate (Sigma), 1% PEG400 (Sigma), and 0.7% benzoyl peroxide
1015 (Polysciences, Inc., Warrington, PA)/acetone until infiltration was complete. The
1016 femurs were then placed on pre-polymerized base layers, covered with freshly
1017 catalyzed MMA embedding solution (for 100 mL, 85mL MMA, 14mL dibutyl
1018 phthalate, 1mL PEG400, 0.33uL DMT, and 0.8g BPO), and incubated under
1019 vacuum until the MMA was polymerized. The polymerized blocks were
1020 trimmed, sequentially polished to a completely smooth surface, and coated with
1021 gold using a sputter coater (Desk V, Denton Vacuum, NJ, USA). Then BSEM (JEOL:
1022 JSM-7800F) was performed to image the osteocyte lacunae on the sectioned
1023 bone surface at 450X magnification starting 2 mm distal from the growth plate.
1024 Six fields from the endosteal and periosteal sides of the cortical bone were taken

1025 as described previously ***Qing and Bonewald*** (***2009***). Using ImageJ (NIH), the
1026 images were thresholded for background removal, binarized, and the lacunar
1027 area from each sample quantitated.

1028 **Mechanical testing using 3-point bending**

1029 Mechanical testing was performed essentially as described in ***Melville et al.***
1030 (***2015***). Briefly, the left femurs were stripped of soft tissue, wrapped in PBS-
1031 soaked gauze, and stored at -20°C until use. Frozen femurs were brought to
1032 room temperature and mounted across the lower supports (8 mm span) of a 3-
1033 point bending platen on a TestResources R100 small force testing machine. The
1034 samples were tested in monotonic bending to failure using a crosshead speed
1035 of 0.05 mm/s. Parameters related to whole bone strength were measured from
1036 force/displacement curves.

1037 **Serum RANKL analysis**

1038 The levels of RANKL were measured in mouse centrifuged serum by using an
1039 ELISA kit (Bio-Techne Corporation, Minneapolis, MN), according to the
1040 manufacturer's protocol.

1041 **Serum parathyroid hormone (PTH) analysis**

1042 Serum was obtained from terminal cardiac puncture and serum PTH levels
1043 were determined using the MicroVue Bone Mouse PTH 1-84 ELISA assay (Quidel
1044 Corp., San Diego, CA) according to the manufacturer's protocol.

1045 **Calcium measurement**

1046 Plasma calcium levels were determined using the Pointe Scientific calcium
1047 Reagent kit (Manufacturer and city). Briefly, diluted serum (1:4 in dH2O) was
1048 incubated with a working calcium color reagent for 1 min and the absorbance
1049 read at 575 nm using a spectrophotometer (BioTek Synergy HTX).

1050 **Sample collection and processing for RNA sequencing**

1051 Bulk RNA sequencing was performed on osteocytes from the control and low
1052 calcium diet, male and female, WT and KO mice. Osteocyte RNA was extracted
1053 from tibia and femur diaphyses after sequential digestion to remove surface cells
1054 including osteoclasts, osteoblasts, and lining cells as previously described ***Qing***
1055 ***et al.*** (***2012***); ***Pin et al.*** (***2022***). Briefly, soft tissue was removed from the bones,
1056 the epiphyses were cut off and bone marrow was removed by flushing with PBS.
1057 The remaining midshafts were incubated at 37°C with 0.2% type 1 collagenase

1058 (Sigma) for 30 minutes, followed by chelation/ digestion in 0.53 mM EDTA/
1059 0.05% trypsin (Cellgro, Mediatech, Inc, Manassas, VA) at 37°C for 30 min
1060 followed by a second collagenase digestion. After each step, the bone chips were
1061 rinsed with PBS and after the final step, flash-frozen in liquid nitrogen, and
1062 pulverized in liquid nitrogen, with Trizol reagent (Qiagen, Carlsbad, CA) added
1063 to the resulting bone powder. Total RNA was isolated with an RNA purification
1064 kit (Qiagen miRNeasy mini kit) and DNase treatment to remove DNA
1065 contamination.

1066 **Library preparation and RNA sequencing**

1067 Total RNA samples were first evaluated for their quantity and quality using
1068 Agilent TapeStation. All the samples used for the sequencing had a RIN of at least
1069 5. 100 nanograms of total RNA were used for library preparation with the KAPA
1070 total RNA Hyperprep Kit (KK8581) (Roche). Each resulting uniquely dual-
1071 indexed library was quantified and quality accessed by Qubit and Agilent
1072 TapeStation. Multiple libraries were pooled in equal molarity. The pooled
1073 libraries were sequenced on an Illumina NovaSeq 6000 sequencer with the v1.5
1074 reagent kit. 100 bp paired-end reads were generated.

1075 **RNA-seq data analysis**

1076 The sequencing reads were first quality-checked using FastQC (v0.11.5,
1077 Babraham Bioinformatics, Cambridge, UK) for quality control. The sequence data
1078 were then mapped to the mouse reference genome mm10 using the RNA-seq
1079 aligner STAR (v2.7.10a) ***Dobin et al.*** (***2013***) with the following parameter: "--
1080 outSAMmapqUnique60". To evaluate the quality of the RNA-seq data, the
1081 number of reads that fell into different annotated regions (exonic, intronic,
1082 splicing junction, intergenic, promoter, UTR, etc.) of the reference genome was
1083 assessed using bamutils ***Breese and Liu*** (***2013***). Uniquely mapped reads were
1084 used to quantify the gene level ex- pression employing featureCounts (subread
1085 v2.0.3) ***Liao et al.*** (***2014***) with the following parameters: "-s 2 -Q 10".

1086 **Quality control of samples**

1087 During data quality control, one of the KO female control samples (sample 23)
1088 was found to have a similar proportion of reads on chromosome Y as in male
1089 mice and a very low expression of the gene Xist, typically highly expressed in
1090 females (Supplementary Figure 3A, 3B), therefore this sample was excluded from
1091 the analysis.

The WT female low-calcium diet samples (samples 16, 17, and 18) had low mapping percentages of 37%, 32%, and 61% respectively. This may be due to bacterial contamination. The two possible methods to process these data are to filter all the possible contaminated reads before alignment or align the reads without filtering. However, filtering the possible contaminated reads before alignment may result in removing some reads from the mouse genome which is similar to the bacterial genome (causing lower gene expression). In contrast, using data without filtering may result in some genes having higher expression levels due to reads from the bacterial genome which are aligned to mice genes. We decided to perform a principal component analysis (PCA) using data without filtering and found that the samples clearly clustered into 4 groups: control male mice, control female mice, low-calcium diet male mice, and low-calcium diet female mice (Supplementary Figure 3C). Within each group, the separation of WT and KO mice is also clear. Due to contamination, samples 16 and 18 were slightly far apart from the others. However, contamination should not have a large global influence on the data as samples 16, 17, and 18 are close to the non-contaminated samples 5 and 6, also in the low-calcium diet female group. Additionally, we validated the data using qPCR with selected genes.

Differentially expressed gene analysis

The read counts matrix was imported to R ***Team*** (***2022***) and analyzed with DEseq2 ***Love et al.*** (***2014***). Within DESeq2, read counts data were normalized with median of ratios, and differentially expressed genes (DEGs) were detected after independent filtering. In DEG analysis, we first detected DEGs between different groups. Significant genes were defined as genes with a p-value less than 0.01 and absolute log2 fold change larger than 1. Gene set enrichment analysis was applied on gene sets from Gene Ontology ***resource: enriching a GOld mine*** (***2021***) using R package clusterProfiler ***Wu*** (***2021***). Several RNA sequencing and pathway figures were prepared with R packages ggplot2 ***Wickham*** (***2016***) and ComplexHeatmap ***Gu*** (***2022***).

Real-time quantitative polymerase chain reaction (qPCR)

Total RNA was reverse transcribed to cDNA using the Verso cDNA Kit (Thermo Fisher Scientific). Transcript levels were measured by real-time PCR (Light Cycler 96; Roche), taking advantage of the TaqMan and Sybr Gene Expression Assay

System (Thermo Fisher Scientific). Expression levels for RANKL (*Tnfsf11*, Forward primer: CCG AGC TGG TGA AGA AAT TAG, Reverse: CCC AAA GTA CGT CGC ATC TTG), Cathepsin K (*Ctsk*, Primer Bank ID: Mm.PT.58.9655974, IDT), TRAP (*Acp5*, Mm.PT.58.5755766, IDT), and sclerostin (*Sost*, Mm00470479_m1, Applied Biosystems) were quantitated. Gene expression was normalized to β-2-microglobulin (*B2m*, Forward: ACA GTT CCA CCC GCC TCA CAT T, Reverse: TAG AAA GAC C A G TCC TTG CTG AAG) levels using the standard $2^{-\Delta\Delta Ct}$ method.

Statistical Analysis

Data are expressed as individual data points. The statistical analysis was done by Prism 8.2 (GraphPad Software, San Diego, CA, USA) and R 4.3.0. When comparing three or more groups with two variables, a two-way repeated-measures analysis of variance (ANOVA) was used with Tukey's post hoc test. To compare between two groups, the unpaired, two-tailed Student's t-test was used. Differences were considered significant at * $p < 0.05$, ** $p < 0.01$, and *** $p < 0.001$.

ACKNOWLEDGEMENTS:

We would like to thank the Center for Medical Genomics, the Small Animal Phenotypic Core, and the Histology and Histomorphometry Core at the Indiana Center for Musculoskeletal Health for help and advice with histological sample preparation. We would like to thank Dr. Yukiko Kitase, Dr. Eijiro Sakamoto, and Carrie Zhao for their help and advice with the experiments. This work was supported by NIH awards P01 AG039355 (to L.F.B).

Disclosures

The authors declare that they have no conflicts of interest.

Data Availability Statement

All data that support the findings of this study are available from the

corresponding author upon reasonable request.

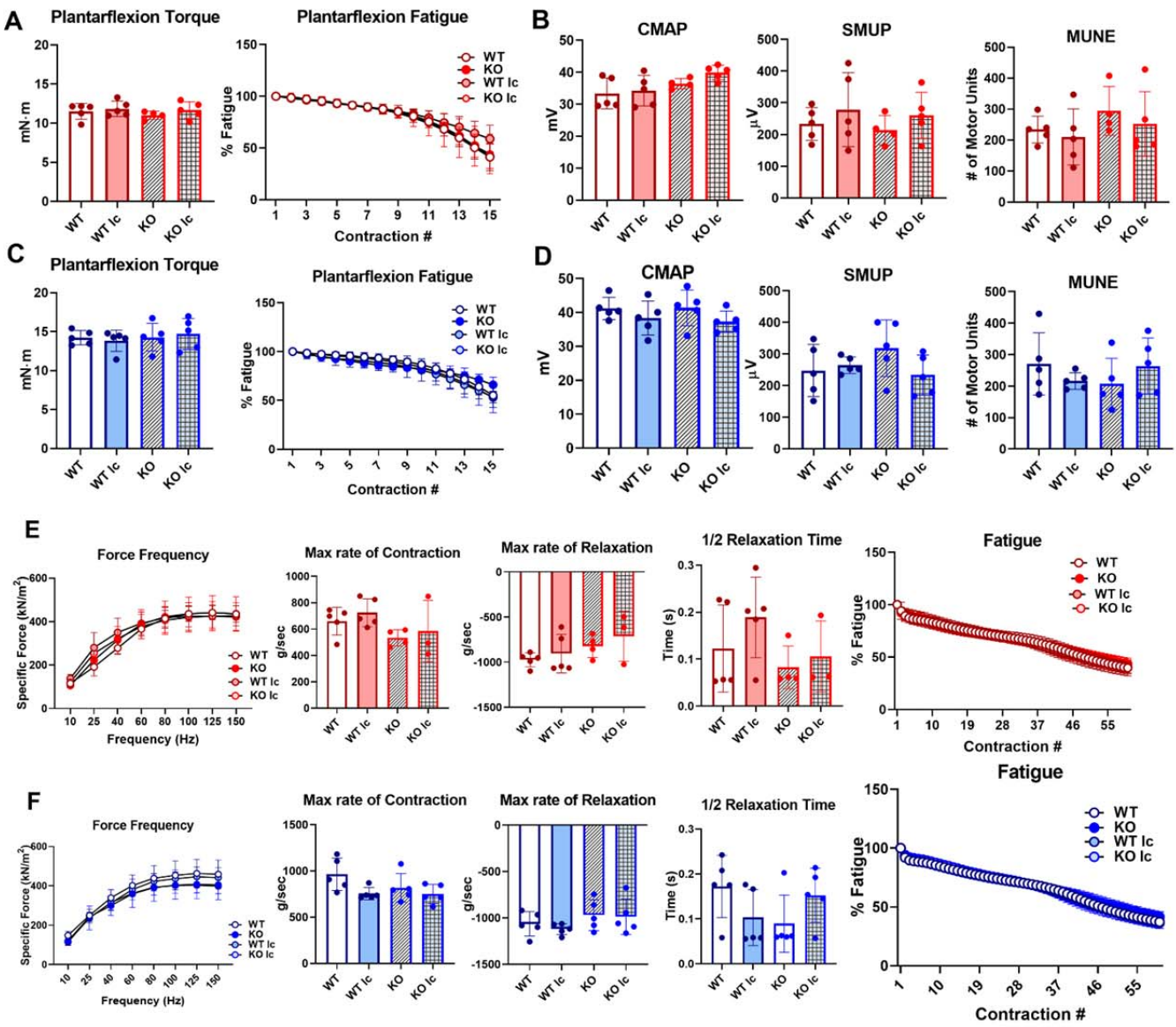

Supplementary Figure 1: Neither genotype nor dietary calcium alters muscle functions *in vivo* or *ex vivo*

Panels A and C show *in vivo* muscle plantarflexion force (reported as plantarflexion torque and plantarflexion fatigue) in WT and KO female (A) and male (C) mice on a control or a low calcium diet, panels B and D show muscle electrophysiology parameters of CMAP, SMUP, and MUNE in WT and KO female (B) and male (D) mice, and panels E and F show *ex vivo* EDL functional measurement (reported as specific force frequency, maximum rate of contraction, maximum rate of relaxation, half-relaxation time, and % fatigue) in WT and KO female (E) and male (F) mice

2-way ANOVA with Tukey's post hoc test was done. n= 4-5/group. As depicted here, red is female,

and blue is male.

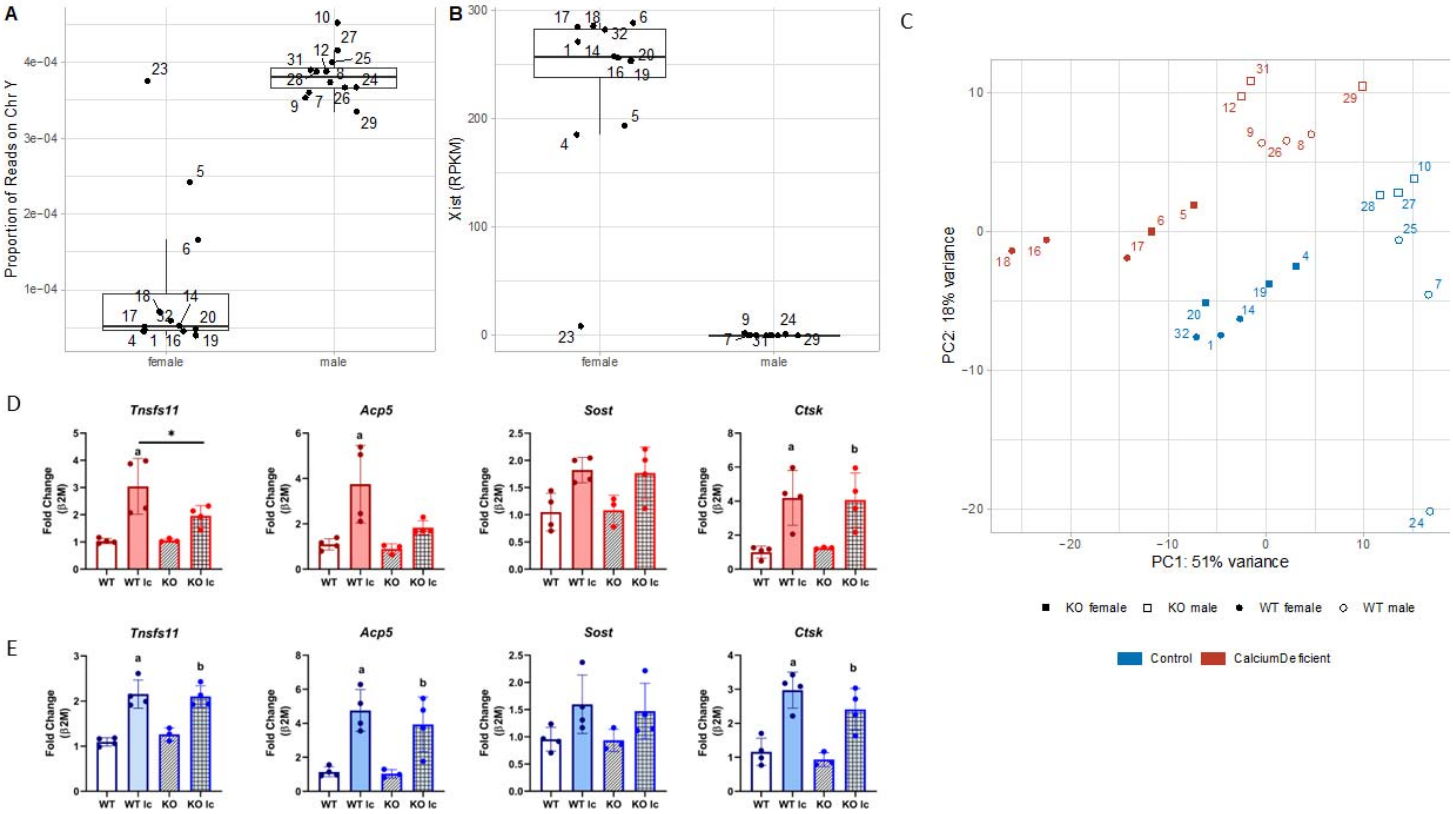

Supplementary Figure 2: Quality control and validation of RNA sequencing

Sanity check of data on the sample's sex. **A:** Boxplot of proportional of reads on chromosome Y. Male should have a higher value than female. **B**: Boxplot of RPKM of Xist. Males should have very low expression of Xist. **C**: Scatter plot of PC1 and PC2 from Principal Component Analysis (PCA) of gene expression data. **D**: qPCR analysis of Tnsfs11, Acp5, Sost, and Ctsk genes from osteocyte-enriched bone chips from female samples. n= 3-4/sample. Two-way ANOVA with Tukey's post-hoc test was performed for statistical analysis. Gene fold-change was normalized using β-2-microglobulin as the housekeeping gene. a= Significantly different from WT, b= Significantly different from KO, *= $p< 0.05$. **E**: qPCR analysis of Tnsfs11, Acp5, Sost, and Ctsk genes from osteocyte-enriched bone chips from male samples. n= 3-4/sample. Two-way ANOVA with Tukey's post-hoc test was performed for statistical analysis. Gene fold-change was normalized using β-2-microglobulin as the housekeeping gene. a= Significantly different from WT, b= Significantly different from KO, *= $p< 0.05$.

Bone Parameters	Virgin		Lactation	
	WT	KO	WT	KO
Femoral cortical bone parameters				
Ct. B. Ar/T. Ar (%)	47.4 ± 1.2	48 ± 1	35.2 ± 1.8[a]	37.5 ± 1.8[b, c]
Ct. Th (mm)	0.18 ± 0.004	0.19 ± 0.005	0.13 ± 0.004[a]	0.14 ± 0.01[b, c]
Ps. Pm (mm)	5.16 ± 0.2	5.2 ± 0.06	5.18 ± 0.16	5.2 ± 0.14
Es. Pm (mm)	3.95 ± 0.1	4 ± 0.13	4.4 ± 0.11[a]	4.3 ± 0.09[b]
Marrow cavity area (mm^2)	0.93 ± 0.1	0.93 ± 0.04	1.16 ± 0.05[a]	1.13 ± 0.05[b]
Femoral trabecular bone parameters				
BV/TV (%)	3.7 ± 1	4.5 ± 0.8	3.1 ± 0.7	4 ± 1.1
Tb. Th (mm)	0.043 ± 0.002	0.044 ± 0.001	0.039 ± 0.002[a]	0.039 ± 0.001[b]
Tb. Sp (mm)	0.37 ± 0.05	0.36 ± 0.03	0.57 ± 0.15[a]	0.44 ± 0.09
Tb. N (1/mm)	0.85 ± 0.2	1.06 ± 0.2	0.8 ±0.2	1.04 ± 0.25

Bone parameters	Change	% Change	
		WT	KO
Cortical Bone Area Fraction	Decrease	26%	22% *
Cortical Thickness	Decrease	29%	24% *
Ultimate Force	Decrease	38%	31% *
Osteoclast Number/ bone parameter	Increase	141%	129%
TRAP-positive osteocytes	Increase	101%	175% *
Lacunar Area	Increase	26%	15% *
Serum RANKL	Increase	170%	80% *

Supplementary Table 1: FNDC5 KO mice femurs are partially resistant to lactation-induced bone loss.

Femoral cortical and trabecular bone parameters of WT and FNDC5 KO female virgin and

lactation mice. n = 5-8/group. a= significant compared to WT control, b= significant compared to KO control, c= significant compared to WT low Ca diet, 2-way ANOVA with Tukey's post hoc test, significance <0.05, n= 8/group. Percentage change in different bone and serum parameters in WT and FNDC5 KO female mice with lactation. *= p<0.05 compared to WT.

Bone Parameters	Female Normal Diet		Female Low Ca Diet		Male Normal Diet		Male Low Ca Diet	
	WT	KO	WT	KO	WT	KO	WT	KO
***Ex vivo* femur DXA**								
BMD (mg/cm^2)	75.4± 2.4	76.6± 1.5	65.4± 4.3[a]	71.4± 3.4 [c]	74.6± 1.5	78.3± 3[a]	68.2± 3	68.1± 2[b]
BMC (g)	0.03± 0.002	0.03± 0.001	0.024± 0.002[a]	0.027± 0.002 [b,c]	0.029± 0.002	0.032± 0.004	0.026± 0.002	0.025± 0.003[b]
Femoral cortical bone parameters								
Ct. B.Ar/T.Ar%	47.8± 1.6	48.4± 0.4	41.6± 1.1[a]	45.2± 1.4[b, c]	40.1± 1.4	43.6± 0.6[a]	38.3± 0.9	39.1± 1.2[b]
Ct. Th (mm)	0.2± 0.01	0.2± 0.01	0.15± 0.01[a]	0.17± 0.01[b, c]	0.15± 0.01	0.2± 0.01[a]	0.14± 0.01	0.14± 0.01[b]
Marrow Cavity Area	0.92 ± 0.04	0.86± 0.02	1.02 ± 0.06[a]	0.9 ± 0.02[c]	1.1 ± 0.04	1.03 ± 0.06[a]	1.2 ± 0.03	1.08 ± 0.03[c]
Femoral trabecular bone parameters								
BV/TV (%)	3.6 ± 1.2	4.3 ± 1	3.2 ± 1	3.9 ± 1	6.1 ± 1.1	8.7 ± 1.9	5.3 ± 1.2	6.4 ± 0.6
Tb. Th (mm)	0.059± 0.002	0.059 ± 0.004	0.056± 0.002	0.055± 0.001	0.036 ± 0.001	0.035 ± 0.001	0.035±0 .001	0.035 ± 0.002
Tb. Sp (mm)	0.38 ± 0.03	0.35 ± 0.02	0.51 ± 0.12[a]	0.48 ± 0.08[b]	0.274 ± 0.025	0.235 ± 0.021	0.278 ± 0.027	0.265 ± 0.01
Tb. N (1/mm)	0.81 ± 0.2	0.95 ± 0.14	0.7 ± 0.02	0.91 ±0.13	1.7 ± 0.34	2.5[a] ± 0.5	1.5 ± 0.3	1.8 ± 0.1
Femoral mechanical properties								
Ultimate	19±	19.4±	14.8±	16.4±	18.3±	17.6±	15±	12.7±

Force (N)	1	1.15	0.7[a]	0.5[b]	1	0.9	1.3[a]	1.5[b, c]
Stiffness (N/mm)	78.6± 3.2	79.1± 4.9	56.8± 5[a]	67± 4.3	76.7± 5.6	56.4± 4.75[a]	56± 10.2[a]	48.5± 4.9[b, c]
Energy to Failure (N)	2.9± 0.3	3.1± 0.6	1.8± 0.5[a]	2± 0.3[b]	3.6± 0.9	3.01± 0.6	2.5± 0.3[a]	2.35± 0.14

Supplementary Table 2: WT and FNDC5 KO female and male mice bone responds differently to a low-calcium diet

Femoral BMD, BMC, cortical and trabecular bone parameters, and mechanical properties of 4-5-month-old WT and KO female and male mice under a normal diet or a 2-week low calcium diet. n = 5/group. a= significant compared to WT control, b= significant compared to KO control, c= significant compared to WT low Ca diet, 2-way ANOVA with Tukey's posthoc test, significance <0.05, n= 4-5/group.

References

Andersson G, Ek-Rylander B, Hollberg K, Ljusberg-Sjölander J, Lång P, Norgård M, Wang Y, Zhang SJ. TRACP as an osteopontin phosphatase. J Bone Miner Res. 2003 J Bone Miner Res. 2003; 18(10):1912–1917.

Ardeshirpour L, Dumitru C, Dann P, Sterpka J, VanHouten J, Kim W, Kostenuik P, Wysolmerski J. OPG Treatment Prevents Bone Loss During Lactation But Does Not Affect Milk Production or Maternal Calcium Metabolism. Endocrinology. 2015; 156(8):2762–73.

Bao JF, She QY, Hu PP, Jia N, Li A. Irisin, a fascinating field in our times. Trends Endocrinol Metab. 2022; 33(9):601– 613.

Bélanger LF. Osteocytic osteolysis. Calcif Tissue Res. 1969; 4(1):1–12.

Body JJ, Terpos E, Tombal B, Hadji P, Arif A, Young A, Aapro M, Coleman R. Bone health in the elderly cancer patient: A SIOG position paper. Cancer Treat Rev. 2016; 51:46–53.

Bonewald L. Use it or lose it to age: A review of bone and muscle communication. Bone. 2019; 120:212–218.

Bonewald LF. The amazing osteocyte. J Bone Miner Res. 2011; 26(2):229–267.

Bostrom P, Wu J, Jedrychowski MP, Korde A, Ye L, Lo JC, Rasbach KA, Boström EA, Choi JH, Long JZ, Kajimura S, Zingaretti MC, Vind BF, Tu H, Cinti S, Højlund K, Gygi SP, Spiegelman BM. A PGC1-alpha-dependent myokine that drives brown-fat-like development of white fat and thermogenesis. Nature. 2012; 481(7382):463–471.

Bouxsein ML, Boyd SK, Christiansen BA, Guldberg RE, Jepsen KJ, Müller R. Guidelines for assessment of bone microstructure in rodents using micro- computed tomography. J Bone Miner Res. 2010; 25(7):1468–86.

Breese MR, Liu Y. NGSUtils: a software suite for analyzing and manipulating next-generation sequencing datasets. Bioinformatics. 2013; 29(4):494–500.

Brotto M, Bonewald L. Bone and muscle: Interactions beyond mechanical. Bone. 2015; 80:109–114.

Celi FS, Brown H. Adipose Tissue Plasticity: Hormonal and Environmental Manipulation, in Hormones. Spiegelman B, editor, Springer Copyright; 2017.

Colaianni G, Cuscito C, Mongelli T, Oranger A, Mori G, Brunetti G, Colucci S, Cinti S, Grano M. Irisin enhances osteoblast differentiation in vitro. Int J Endocrinol. 2014; p. 902186–902186.

1283 **Colaianni G**, Cuscito C, Mongelli T, Pignataro P, Buccoliero C, Liu P, Lu P, Sartini L, Di
1284 Comite M, Mori G, Di Benedetto A, Brunetti G, Yuen T, Sun L, Reseland JE, Colucci S, New
1285 MI, Zaidi M, Cinti S, Grano M. The myokine irisin increases cortical bone mass. Proc Natl
1286 Acad Sci. 2015; 112(39):12157–62.

1287 **Colaianni G**, Mongelli T, Cuscito C, Pignataro P, Lippo L, Spiro G, Notarnicola A, Severi I, Passeri G,
1288 Mori G, Brunetti G, Moretti B, Tarantino U, Colucci SC, Reseland JE, Vettor R, Cinti S, Grano M. Irisin
1289 prevents and restores bone loss and muscle atrophy in hind-limb suspended mice. Sci Rep, 2017;
1290 7(1): p. 2811.

1291 **Colaianni G**, Grano M. Role of Irisin on the bone-muscle functional unit. Bonekey Rep, 2015; 4: p.
1292 765.

1293 **Colucci SC**, Buccoliero C, Sanesi L, Errede M, Colaianni G, Annese T, Khan MP, Zerlotin
1294 R, Dicarlo M, Schipani E, Kozloff KM, Grano M. Systemic Administration of Recombinant
1295 Irisin Accelerates Fracture Healing in Mice. Int J Mol Sci. 2019; p. 22–22.

1296 **Dallas SL**, Prideaux M, Bonewald LF. The osteocyte: an endocrine cell ... and more. Endocr
1297 Rev. 2013; 34(5):658–90.

1298 **Dobin A,** Davis CA, Schlesinger F, Drenkow J, Zaleski C, Jha S, Batut P, Chaisson M,
1299 Gingeras TR. STAR: ultrafast universal RNA-seq aligner. Bioinformatics. 2013; 29(1):15–21.

1300 **During A**. Osteoporosis: A role for lipids. Biochimie. 2020; 178:49–55.

1301 **Erickson HP**. Irisin and FNDC5 in retrospect: An exercise hormone or a transmembrane receptor?
1302 Adipocyte, 2013; 2(4): p. 289-93.

1303 **Essex AL,** Huot JR, Deosthale P, Wagner A, Figueras J, Davis A, Damrath J, Pin F, Wallace J,
1304 Bonetto A, Plotkin LI. Triggering Receptor Expressed on Myeloid Cells 2 (TREM2) R47H
1305 Variant Causes Distinct Age- and Sex-Dependent Musculoskeletal Alterations in Mice. J Bone
1306 Miner Res. 2022; 37(7):1366–1381.

1307 **Estell EG**, Le PT, Vegting Y, Kim H, Wrann C, Bouxsein ML, Nagano K, Baron R,
1308 Spiegelman BM, Rosen CJ. Irisin directly stimulates osteoclastogenesis and bone
1309 resorption in vitro and in vivo. Elife. 2020; p. 2020–2029.

1310 **Farley JR**, Baylink DJ. Skeletal alkaline phosphatase activity as a bone formation index in
1311 vitro. Metabolism. 1986; 35(6):563–71.

1312 **Feng JQ**, Ye L, Schiavi S. Do osteocytes contribute to phosphate homeostasis? Curr Opin
1313 Nephrol Hypertens. 2009; 18(4):285–91.

1314 **Geng W**, Wright GL. Skeletal sensitivity to dietary calcium deficiency is increased in the
1315 female compared with the male rat. Can J Physiol Pharmacol. 2001; 79(5):379–85.

1316 **The Gene Ontology Resource: enriching a GOld mine TGO**. Nucleic Acids Res.
1317 2021; 49(D1):325–334.

1318 **Goltzman D**. Studies on the mechanisms of the skeletal anabolic action of endogenous
1319 and exogenous parathyroid hormone. Arch Biochem Biophys. 2008; 473(2):218–242.

1320 **Gu Z**. Complex heatmap visualization. iMeta, 2022; 1(3): p. e43.

1321 **Hamrick MW**, Samaddar T, Pennington C, McCormick J. Increased muscle mass with
1322 myostatin deficiency improves gains in bone strength with exercise. J Bone Miner Res.
1323 2006; 21(3):477–83.

1324 **Huot JR,** Pin F, Essex AL, Bonetto A. MC38 Tumors Induce Musculoskeletal Defects in
1325 Colorectal Cancer. Int J Mol Sci. 2021; 22(3).

1326 **Huot JR**, Pin F, Chatterjee R, Bonetto A. PGC1α overexpression preserves muscle mass
1327 and function in cisplatin-induced cachexia. J Cachexia Sarcopenia Muscle. 2022;
1328 13(5):2480–2491.

1329 **Islam MR,** Valaris S, Young MF, Haley EB, Luo R, Bond SF, Mazuera S, Kitchen RR,
1330 Caldarone BJ, Bettio LEB, Christie BR, Schmider AB, Soberman RJ, Besnard A,
1331 Jedrychowski MP, Kim H, Tu H, Kim E, Choi SH, Tanzi RE, Spiegelman BM, Wrann CD.
1332 Exercise hormone irisin is a critical regulator of cognitive function. Nat Metab. 2021;
1333 (8):1058–1070.

1334 **Jahn K**, Kelkar S, Zhao H, Xie Y, Tiede-Lewis LM, Dusevich V, Dallas SL, Bonewald LF.
1335 Osteocytes Acidify Their Microenvironment in Response to PTHrP In Vitro and in
1336 Lactating Mice In Vivo. J Bone Miner Res. 2017; 32(8):1761–1772.

1337 **Jähn-Rickert K**, Zimmermann EA. Potential Role of Perilacunar Remodeling in the
1338 Progression of Osteoporosis and Implications on Age-Related Decline in Fracture
1339 Resistance of Bone. Curr Osteoporos Rep. 2021; 19(4):391–402.

1340 **Jo D**, Song J. Irisin Acts via the PGC-1α and BDNF Pathway to Improve Depression-like
1341 Behavior. Clin Nutr Res. 2021; 10(4):292–302.

1342 **Johannesdottir F**, Aspelund T, Reeve J, Poole KE, Sigurdsson S, Harris TB, Gudnason VG,
1343 Sigurdsson G. Similarities and differences between sexes in regional loss of cortical and
1344 trabecular bone in the mid-femoral neck: the AGES-Reykjavik longitudinal study. J Bone
1345 Miner Res. 2013; 28(10):2165–76.

1346 **Johnston CB**, Dagar M. Osteoporosis in Older Adults. Med Clin North Am. 2020;
1347 104(5):873–884.

1348 **Kalkwarf HJ**. Lactation and maternal bone health. Adv Exp Med Biol. 2004; 554:101–115.

Kaplan MM. Alkaline phosphatase. N Engl J Med. 1972; 286(4):200–202.

Karsenty G, Mera P. Molecular bases of the crosstalk between bone and muscle. Bone. 2018; 115:43–49.

Kawao N, Moritake A, Tatsumi K, Kaji H. Roles of Irisin in the Linkage from Muscle to Bone During Mechanical Unloading in Mice. Calcif Tissue Int. 2018; 103(1):24–34.

Kim H, Wrann CD, Jedrychowski M, Vidoni S, Kitase Y, Nagano K, Zhou C, Chou J, Parkman VA, Novick SJ, Strutzenberg TS, Pascal BD, Le PT, Brooks DJ, Roche AM, Gerber KK, Mattheis L, Chen W, Tu H, Bouxsein ML, Griffin PR, Baron R, Rosen CJ, Bonewald LF, Spiegelman BM. Irisin Mediates Effects on Bone and Fat via alphaV Integrin Receptors. Cell. 2018; 175(7):17–17.

Kitase Y, Vallejo JA, Gutheil W, Vemula H, Jähn K, Yi J, Zhou J, Brotto M, Bonewald LF. *β*-aminoisobutyric Acid, l-BAIBA, Is a Muscle-Derived Osteocyte Survival Factor. Cell Rep. 2018; 22(6):1531–1544.

Korta P, Pocheć E, Mazur-Biały A. Irisin as a Multifunctional Protein: Implications for Health and Certain Diseases. Medicina (Kaunas), 2019; 55(8).

Kovacs CS. Calcium and bone metabolism in pregnancy and lactation. The Journal of clinical endocrinology and metabolism. 2001; (6):86–86.

Kumssa DB, Joy EJ, Ander EL, Watts MJ, Young SD, Walker S, Broadley MR. Dietary calcium and zinc deficiency risks are decreasing but remain prevalent. Sci Rep, 2015; 5: p. 10974.

Kurapaty SS, Hsu WK. Sex-Based Difference in Bone Healing: A Review of Recent Preclinical Literature. Curr Rev Musculoskelet Med. 2022.

Lee HJ, Lee JO, Kim N, Kim JK, Kim HI, Lee YW, Kim SJ, Choi JI, Oh Y, Kim JH, Suyeon-Hwang, Park SH, Kim HS. Irisin, a Novel Myokine, Regulates Glucose Uptake in Skeletal Muscle Cells via AMPK. Mol Endocrinol. 2015; 29(6):873–81.

Liao Y, Smyth GK, Shi W. featureCounts: an efficient general purpose program for assigning sequence reads to genomic features. Bioinformatics. 2014; 30(7):923–953.

Liu Q, Lei L, Yu T, Jiang T, Kang Y. Effect of Brain-Derived Neurotrophic Factor on the Neurogenesis and Osteogenesis in Bone Engineering. Tissue Eng Part A. 2018; 24:1283–1292.

Love MI, Huber W, Anders S. Moderated estimation of fold change and dispersion for RNA-seq data with DESeq2. Genome Biol. 2014; 15(12):550–550.

Lu D, Demissie S, Horowitz NB, Gower AC, Lenburg ME, Alekseyev YO, Hussein AI, Bragdon B, Liu Y,

Daukss D, Page JM, Webster MZ, Schlezinger JJ, Morgan EF, Gerstenfeld LC. Temporal and Quantitative Transcriptomic Differences Define Sexual Dimorphism in Murine Postnatal Bone Aging. JBMR Plus, 2022; 6(2): p. e10579.

Luo X, Li J, Zhang H, Wang Y, Shi H, Ge Y, Yu X, Wang H, Dong Y. Irisin promotes the browning of white adipocytes tissue by AMPKα1 signaling pathway. Res Vet Sci. 2022; 152:270–276.

Ma Y, Qiao X, Zeng R, Cheng R, Zhang J, Luo Y, Nie Y, Hu Y, Yang Z, Zhang J, Liu L, Xu W, Xu CC, Xu L. Irisin promotes proliferation but inhibits differentiation in osteoclast precursor cells. Faseb j. 2018; p. 201700983–201700983.

Maak S, Norheim F, Drevon CA, Erickson HP. Progress and Challenges in the Biology of FNDC5 and Irisin. Endocr Rev. 2021; 42(4):436–456.

Matikainen N, Pekkarinen T, Ryhänen EM, Schalin-Jäntti C. Physiology of Calcium Homeostasis: An Overview. Endocrinol Metab Clin North Am. 2021; 50(4):575–590.

Melville KM, Robling AG, Meulen MCVD. In vivo axial loading of the mouse tibia. Methods Mol Biol. 2015; 1226:99–115.

Mo C, Zhao R, Vallejo J, Igwe O, Bonewald L, Wetmore L, Brotto M. Prostaglandin E2 promotes proliferation of skeletal muscle myoblasts via EP4 receptor activation. Cell Cycle. 2015; 14(10):1507–1523.

Moreno-Layseca P, Icha J, Hamidi H, Ivaska J. Integrin trafficking in cells and tissues. Nat Cell Biol. 2019; 21(2):122– 132.

Mu A, Wales TE, Zhou H, Draga-Coletă SV, Gorgulla C, Blackmore KA, Mittenbühler MJ, Kim CR, Bogoslavski D, Zhang Q, Wang ZF, Jedrychowski MP, Seo HS, Song K, Xu AZ, Sebastian L, Gygi SP, Arthanari H, Dhe-Paganon S, Griffin PR, Engen JR, Spiegelman BM. Irisin acts through its integrin receptor in a two-step process involving extracellular Hsp90α. Mol Cell. 2023; 83(11):1903–1920.

Muruganandan S, Sinal CJ. The impact of bone marrow adipocytes on osteoblast and osteoclast differentiation. IUBMB Life. 2014; 66(3):147–155.

Nakashima T, Hayashi M, Fukunaga T, Kurata K, Oh-Hora M, Feng JQ, Bonewald LF, Kodama T, Wutz A, Wagner EF, Penninger JM, Takayanagi H. Evidence for osteocyte regulation of bone homeostasis through RANKL expression. Nat Med. 2011; 17(10):1231–1235.

Ono T, Hayashi M, Sasaki F, Nakashima T. RANKL biology: bone metabolism, the immune system, and beyond. Inflamm Regen, 2020; 40: p. 2.

1414 **Osipov B**, Paralkar MP, Emami AJ, Cunningham HC, Tjandra PM, Pathak S, Langer HT, Baar
1415 K, Christiansen BA. Sex differences in systemic bone and muscle loss following femur
1416 fracture in mice. J Orthop Res. 2022; (4):878–890.

1417 **Perakakis N**, Triantafyllou GA, Fernández-Real JM, Huh JY, Park KH, Seufert J,
1418 Mantzoros CS. Physiology and role of irisin in glucose homeostasis. Nat Rev
1419 Endocrinol. 2017; 13(6):324–337.

1420 **Pin F,** Prideaux M, Huot JR, Essex AL, Plotkin LI, Bonetto A, Bonewald LF. Non-bone
1421 metastatic cancers promote osteocyte-induced bone destruction. Cancer Lett. 2021;
1422 520:80–90.

1423 **Pin F,** Jones AJ, Huot JR, Narasimhan A, Zimmers TA, Bonewald LF, Bonetto A. RANKL
1424 Blockade Reduces Cachexia and Bone Loss Induced by Non-Metastatic Ovarian
1425 Cancer in Mice. J Bone Miner Res. 2022; 37(3):381–396.

1426 **Posa F**, Colaianni G, Di Cosola M, Dicarlo M, Gaccione F, Colucci S, Grano M, Mori G.
1427 The Myokine Irisin Promotes Osteogenic Differentiation of Dental Bud-Derived MSCs.
1428 Biology. 2021;(4).

1429 **Qi JY**, Yang LK, Wang XS, Wang M, Li XB, Feng B, Wu YM, Zhang K, Liu SB. Irisin: A
1430 promising treatment for neurodegenerative diseases. Neuroscience. 2022; 498:289–299.

1431 **Qing H,** Ardeshirpour L, Pajevic PD, Dusevich V, Jähn K, Kato S, Wysolmerski J,
1432 Bonewald LF. Demonstration of osteocytic perilacunar/canalicular remodeling in mice
1433 during lactation. J Bone Miner Res. 2012; 27(5):1018–1047.

1434 **Qing H**, Bonewald LF. Osteocyte remodeling of the perilacunar and pericanalicular matrix.
1435 International Journal of Oral Science. 2009.

1436 **Robling AG**, Bonewald LF. The Osteocyte: New Insights. Annu Rev Physiol. 2020; 82:485–
1437 506.

1438 **Rosen CJ**, Bouxsein ML. Mechanisms of disease: is osteoporosis the obesity of bone? Nat
1439 Clin Pract Rheumatol. 2006; 2(1):35–43.

1440 **Saedi A**, Bermeo S, Plotkin L, Myers DE, Duque G. Mechanisms of palmitate-induced
1441 lipotoxicity in osteocytes. Bone. 2019; 127:353–359.

1442 **Saedi A**, Chen L, Phu S, Vogrin S, Miao D, Ferland G, Gaudreau P, Duque G. Age-Related
1443 Increases in Marrow Fat Volumes have Regional Impacts on Bone Cell Numbers and
1444 Structure. Calcif Tissue Int. 2020; 107(2):126–134.

1445 **Schwartz AV**. Marrow fat and bone: review of clinical findings. Front Endocrinol (Lausanne), 2015;
1446 6: p. 40.

1447 **Sharma A**, Michels LV, Pitsillides AA, Greeves J, Plotkin LI, Cardo V, Sims NA, Clarkin CE.
1448 Sexing Bones: Improving Transparency of Sex Reporting to Address Bias Within
1449 Preclinical Studies. J Bone Miner Res. 2023; 38(1):5–13.

1450 **Shimonty A**, Bonewald LF, Pin F. Role of the Osteocyte in Musculoskeletal Disease. Curr
1451 Osteoporos Rep. 2023; 21(3):303–310.

1452 **Silver IA**, Murrills RJ, Etherington DJ. Microelectrode studies on the acid microenvironment
1453 beneath adherent macrophages and osteoclasts. Exp Cell Res. 1988; 175(2):266–76.

1454 **Styner M**, Pagnotti GM, Galior K, Wu X, Thompson WR, Uzer G, Sen B, Xie Z, Horowitz
1455 MC, Styner MA, Rubin C, Rubin J.Exercise Regulation of Marrow Fat in the Setting of
1456 PPARμ Agonist Treatment in Female C57BL/6 Mice. Endocrinology. 2015;
1457 156(8):2753–61.

1458 **Team RC**. R: A Language and Environment for Statistical Computing. 2022, R Foundation
1459 for Statistical Computing. In: 2022.

1460 **Temiyasathit S**, Jacobs CR. Osteocyte primary cilium and its role in bone
1461 mechanotransduction. Ann N Y Acad Sci. 2010; 1192:422–430.

1462 **Teti A**, Zallone A. Do osteocytes contribute to bone mineral homeostasis? Osteocytic
1463 osteolysis revisited. Bone. 2009; 44(1):11–17.

1464 **Tsourdi E**, Jähn K, Rauner M, Busse B, Bonewald LF. Physiological and pathological osteocytic
1465 osteolysis. J Musculoskelet Neuronal Interact. 2018; 18(3):292–303.

1466 **Tsourdi E**, Anastasilakis AD, Hofbauer LC, Rauner M, Lademann F. Irisin and Bone in
1467 Sickness and in Health: A Narrative Review of the Literature. J Clin Med. 2022; (22):11–
1468 11.

1469 **Uda Y**, Azab E, Sun N, Shi C, Pajevic PD. Osteocyte Mechanobiology. Curr Osteoporos Rep,
1470 2017; 15(4): p. 318-325.

1471 **Wang H**, Zhao YT, Zhang S, Dubielecka PM, Du J, Yano N, Chin YE, Zhuang S, Qin G, Zhao
1472 TC. Irisin plays a pivotal role to protect the heart against ischemia and reperfusion
1473 injury. J Cell Physiol. 2017; 232(12):3775–3785.

1474 **Wickham H**. GGPLOT2: Elegant Graphics for Data Analysis. New York: Springer-Verlag;
1475 2016.

1476 **Wrann CD**, White JP, Salogiannnis J, Laznik-Bogoslavski D, Wu J, Ma D, Lin JD, Greenberg
1477 ME, Spiegelman BM. Exercise induces hippocampal BDNF through a PGC-1α/FNDC5
1478 pathway. Cell Metab. 2013; 18(5):649–59.

1479 **Wu T**. clusterProfiler 4.0: A universal enrichment tool for interpreting omics data. Innovation

(Camb), 2021; 2(3): p. 100141.

Wysolmerski JJ. The evolutionary origins of maternal calcium and bone metabolism during lactation. J Mammary Gland Biol Neoplasia. 2002; 7(3):267–76.

Wysolmerski JJ. Osteocytic osteolysis: time for a second look? Bonekey Rep, 2012; 1: p. 229.

Wysolmerski JJ. Osteocytes remove and replace perilacunar mineral during reproductive cycles. Bone. 2013; 54(2):230–236.

Xin C, Liu J, Zhang J, Zhu D, Wang H, Xiong L, Lee Y, Ye J, Lian K, Xu C, Zhang L, Wang Q, Liu Y, Tao L. Irisin improves fatty acid oxidation and glucose utilization in type 2 diabetes by regulating the AMPK signaling pathway. Int J Obes. 2016; 40(3):443–51.

Xiong J, Piemontese M, Onal M, Campbell J, Goellner JJ, Dusevich V, Bonewald L, Manolagas SC, O'Brien CA. Osteocytes, not Osteoblasts or Lining Cells, are the Main Source of the RANKL Required for Osteoclast Formation in Remodeling Bone. PLoS One. 2015; 10(9):138189– 138189.

Xiong J, O'Brien CA. Osteocyte RANKL: new insights into the control of bone remodeling. J Bone Miner Res. 2012; 27(3):499–505.

Yeung DK, Griffith JF, Antonio GE, Lee FK, Woo J, Leung PC. Osteoporosis is associated with increased marrow fat content and decreased marrow fat unsaturation: a proton MR spectroscopy study. J Magn Reson Imaging. 2005; 22(2):279–85.

Youlten SE, Kemp JP, Logan JG, Ghirardello EJ, Sergio CM, Dack MRG, Guilfoyle SE, Leitch VD, Butterfield NC, Komla-Ebri D, Chai RC, Corr AP, Smith JT, Mohanty ST, Morris JA, McDonald MM, Quinn JMW, McGlade AR, Bartonicek N, Jansson M, Hatzikotoulas K, Irving MD, Beleza-Meireles A, Rivadeneira F, Duncan E, Richards JB, Adams DJ, Lelliott CJ, Brink R, Phan TG, Eisman JA, Evans DM, Zeggini E, Baldock PA, Bassett JHD, Williams GR, Croucher PI. Osteocyte transcriptome mapping identifies a molecular landscape control- ling skeletal homeostasis and susceptibility to skeletal disease. Nat Commun. 2021; 12(1):2444–2444.

Young MF, Valaris S, Wrann CD. A role for FNDC5/Irisin in the beneficial effects of exercise on the brain and in neurodegenerative diseases. Prog Cardiovasc Dis. 2019; 62(2):172–178.

Zhang D, Bae C, Lee J, Lee J, Jin Z, Kang M, Cho YS, Kim JH, Lee W, Lim SK. The bone anabolic effects of irisin are through preferential stimulation of aerobic glycolysis. Bone. 2018; 114:150–160.

Zhang H, Wu X, Liang J, Kirberger M, Chen N. Irisin, an exercise-induced bioactive peptide beneficial for health promotion during aging process. Ageing Res Rev. 2022;

1514 80:101680–101680.

1515 **Zhang Y**, Li R, Meng Y, Li S, Donelan W, Zhao Y, Qi L, Zhang M, Wang X, Cui T, Yang LJ,
1516 Tang D. Irisin stimulates browning of white adipocytes through mitogen-activated
1517 protein kinase p38 MAP kinase and ERK MAP kinase signaling. Diabetes. 2014; 63(2):514–
1518 539.

1519 **Zhu J**, Li J, Yao T, Li T, Chang B, Yi X. Analysis of the role of irisin receptor signaling in
1520 regulating osteogenic/adipogenic differentiation of bone marrow mesenchymal stem
1521 cells. Biotechnol Genet Eng Rev. 2023; p. 1–24.